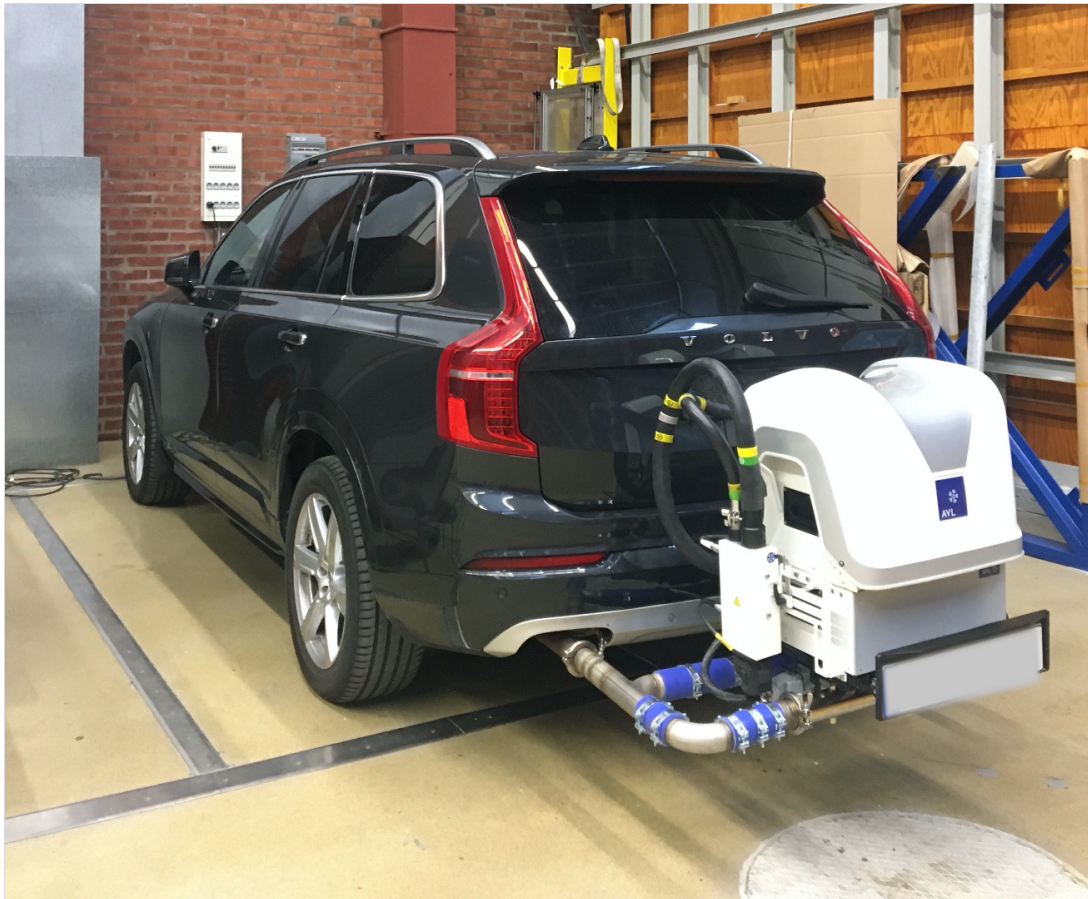




CHALMERS



Real Driving Particulate Emissions from a Gasoline PHEV

Master's thesis in AUTOMOTIVE ENGINEERING

SAHIL SANJAY PATEL
JIDAPA ASAKIT

MASTER'S THESIS IN AUTOMOTIVE ENGINEERING

Real Driving Particulate Emissions from a Gasoline PHEV

SAHIL SANJAY PATEL
JIDAPA ASAKIT

Department of Mechanics and Maritime Sciences
Division of Combustion and Propulsion
CHALMERS UNIVERSITY OF TECHNOLOGY
Göteborg, Sweden 2020

Real Driving Particulate Emissions from a Gasoline PHEV
SAHIL SANJAY PATEL
JIDAPA ASAKIT

© SAHIL SANJAY PATEL , JIDAPA ASAKIT, 2020

Master's thesis 2020:60
Department of Mechanics and Maritime Sciences
Division of Combustion and Propulsion
Chalmers University of Technology
SE-412 96 Göteborg
Sweden
Telephone: +46 (0)31-772 1000

Cover:
The PEMS unit mounted on the tow-bar along with modified exhaust pipe of the test vehicle

Chalmers Reproservice
Göteborg, Sweden 2020

Real Driving Particulate Emissions from a Gasoline PHEV
Master's thesis in AUTOMOTIVE ENGINEERING
SAHIL SANJAY PATEL
JIDAPA ASAKIT
Department of Mechanics and Maritime Sciences
Division of Combustion and Propulsion
Chalmers University of Technology

ABSTRACT

The gasoline Plug-In Hybrid Electric Vehicle (PHEV) has rapidly taken over the majority of the market share in terms of vehicle production and sales due to its reduced emission of exhaust pollutants and increased overall efficiency. This has augmented the importance of studying these emission levels, their behaviour and impact under real-world conditions. This study focuses on local tailpipe emissions such as NO_x , particle number and size from a Gasoline PHEV. The study describes a Real Driving Emissions measurement of a gasoline PHEV in a test cell and on-road using a Portable Emissions Measurement System (PEMS). The measurement instruments used for this study are an AVL PEMS unit and Cambustion's DMS500 Fast Particulate Analyser. Similar amounts of PN from test-cell testings for the PEMS and DMS were found. A particle diameter study showed how the average size of particles emitted varies in the urban, rural and motorway sections. It has to be noted that the test vehicle used for this study does not qualify with on-road legislation. It is also concluded that numerous tests have to be carried out to obtain consistency and repeatability in test results to strengthen claims about the emission behaviour. The measurement capability of instruments used also plays an imminent role in this analysis as noticed with the test-cell data comparison between the PEMS and DMS systems.

Keywords: Real Driving Emissions, Portable Emissions Measurement System, Gasoline Plug-in Hybrid Electric Vehicle, Particulate Emissions

ACKNOWLEDGEMENTS

We wish to express our sincere appreciation to our supervisor, Professor Jonas Sjöblom, who has guided us through every obstacle and encouraged us to be professional and do the right thing even when the road got tough. Without his expert knowledge, the goal of this project would not have been realized. We would like to thank our Head of Division, Dr Lucien Koopmans, for facilitating the test vehicle for our thesis and his constant support both technically and financially.

We would like to extend our gratitude towards Rickard Arvidsson of Volvo Cars, Research Engineer, Robert Buadu, Senior Research Engineer, Alf Magnusson and PhD student, Sreelekha Etikyala for their constant guidance and support throughout the research period.

Further, we acknowledge the Department of Mechanics and Maritime Sciences and Chalmers University of Technology for their resourceful and administrative support. We also thank the AVL support team for the technical support of their instruments used in this research.

Nomenclature

List of Abbreviations

<i>BEV</i>	Battery Electric Vehicle
<i>CAN</i>	Controller Area Network
<i>CF</i>	Conformity Factor
<i>CH₄</i>	Methane
<i>CO</i>	Carbon Monoxide
<i>EATS</i>	Exhaust After Treatment Systems
<i>ECU</i>	Electronic Control Unit
<i>EEA</i>	European Environment Agency
<i>EFM</i>	Exhaust Flow Meter
<i>EV</i>	Electric Vehicle
<i>GDI</i>	Gasoline Direct Injection
<i>GHG</i>	Greenhouse Gas
<i>GPF</i>	Gasoline Particulate Filter
<i>GPS</i>	Global Positioning System
<i>GUI</i>	Graphic User Interface
<i>H₂O</i>	Hydrogen Dioxide
<i>HC</i>	Hydrocarbon
<i>HEV</i>	Hybrid Electric Vehicle
<i>ICE</i>	Internal Combustion Engine
<i>LCA</i>	Life Cycle Assessment
<i>LEZ</i>	Low Emission Zone
<i>LHV</i>	Lower Heating Value
<i>LNG</i>	Liquefied Natural Gas
<i>MAW</i>	Moving Average Window
<i>NDIR</i>	Non-dispersive Infrared Analyser
<i>NDUV</i>	Non-dispersive Ultraviolet Analyser
<i>NEDC</i>	New European Driving Cycle
<i>NG</i>	Natural Gas
<i>NMHC</i>	Non-methane Hydrocarbon
<i>NO_x</i>	Oxides of Nitrogen (NO, NO ₂)
<i>NTE</i>	Not-to-exceed
<i>OBD</i>	On-Board Diagnostics
<i>PEMS</i>	Portable Emission Measurement System
<i>PHEV</i>	Plug-in Hybrid Electric Vehicle
<i>PM</i>	Particulate Matter
<i>PN</i>	Particle Number
<i>PPM</i>	Parts-per-million
<i>PSD</i>	Particle Size Distribution
<i>RDE</i>	Real Driving Emissions
<i>RPA</i>	Relative Positive Acceleration

<i>RPM</i>	Revolutions Per Minute
<i>SI</i>	Spark Ignition
<i>SO₂</i>	Sulphur Dioxide
<i>SoC</i>	State of Charge
<i>THC</i>	Total Hydrocarbon
<i>TWC</i>	Three-Way Catalyst
<i>UFP</i>	Ultra-fine Particles
<i>VPR</i>	Volatile Particle Remover
<i>WLTC</i>	Worldwide Harmonized Vehicle Test Cycle
<i>WLTP</i>	Worldwide Harmonized Vehicle Test Procedure

List of Symbols

\dot{m}	Fuel rate	g/s
\dot{V}	Volume ratio of exhaust system	m^3
ρ_{exh}	Exhaust gas density	kg/m^3
τ	Residence time	s
f_u, f_r, f_m	Weighting factors for urban, rural and motorway shares	
M_{gas}	Mass or particle number of the exhaust component	g/km or #/km
MW_{exh}	Molecular Weight of exhaust gas	kg/kmol
p_{atm}	Ambient pressure	Pa
u_{gas}	component specific factor or ratio of density between densities of gas component and exhaust gas	-
V_{catalyst}	Volume of catalyst	m^3
V_{muffler}	Volume of muffler	m^3
V_{sys}	Volume of exhaust system	m^3
v_{apos95}	Measure of driver aggressiveness	m^2/s^3
R	Universal gas constant	J/mol/K

CONTENTS

Abstract	i
Acknowledgements	i
Contents	v
1 Introduction	1
2 Background	2
2.1 Emission Standards	4
2.1.1 European Emission Standards	4
2.2 Emission Test Procedures	6
2.2.1 New European Driving Cycle (NEDC)	6
2.2.2 World Harmonised Light Vehicles Test Procedure (WLTP)	6
2.2.3 Real Driving Emissions (RDE)	7
3 Methodology	9
3.1 Test Vehicle	9
3.2 Portable Emissions Measurement System (PEMS)	10
3.2.1 PEMS Working Principle	11
3.2.2 Instrument Layout And Measurement Principle Inside PEMS	12
3.2.3 AVL M.O.V.E System Control	14
3.3 DMS500 Mk II Particle Analyser	17
3.4 ETAS INCA	17
3.5 RDE Routes	17
4 RDE Experiment	19
4.1 In-cell Testing	19
4.2 On-road Testing	19
5 Results and Discussions	20
5.1 Summary of results of all tests	20
5.2 Standard Driving Cycle WLTC	23
5.3 RDE: NO _x	25
5.4 RDE: Particle Number	27
5.4.1 Behaviour of Particle Number	27
5.4.2 Comparison between PEMS and DMS500	29
5.4.3 Particle Size Distribution	31
5.4.4 Comparison of On-road and In-cell RDE	35
5.5 Effects of Driving Aggressiveness	37
5.6 Residence Time	39
6 Conclusion	41
References	42
A Appendix	44
A.1 Discussion On Measurement Error In Test-cell	44
A.2 Abnormal behaviour in PEMS PN measurement	46
A.3 Residence time	48
A.4 Standard Cycle WLTC	50
A.4.1 NO _x	50
A.5 Emissions of Flat 1 Route	50
A.5.1 Particle Number	51

A.6 Aggressiveness	52
A.7 Additional Data	53
A.8 Particle size distribution	54

1 Introduction

The world as we perceive it is rapidly evolving and with the focus on climate change we must take steps to act on it. In recent times with the rise in pollution, the well-being of the air we breathe has become a more prominent issue than ever before. One of the many reasons that have led to it is the transportation industry, motor vehicles in particular. According to the European Environment Agency (EEA), the transportation sector including aviation is responsible for 27% of the EU greenhouse gas (GHG) emissions of which road transportation is the major contributor [**TotalEurope**]. Hence, car manufacturers have been targeting to lower GHG emissions by developing new technologies and methods to achieve the goal. A recent new alternative with a promising future is a hybrid or fully electric powertrain. With a hybrid powertrain, Internal Combustion Engine (ICE) and transmission are integrated with electric motor-generators, thus switching between ICE and electric motor to utilize power on different vehicle modes or driving conditions. Therefore, with this, the usage of the combustion engine is drastically diminished and results in lowered exhaust emissions.

In the past, exhaust systems in vehicles had poor conversion efficiency and their importance was less. This was because the emissions regulations were lenient, in contrary to the present regulations. The exhaust emissions from the engine are treated by the Exhaust After-Treatment Systems (EATS) before being released into the environment. Generally, the EATS consists of a catalyst and a particulate filter combination that treat the exhaust gases. The performance of the EATS is heavily dependent on its operating temperature and its configuration that is, the type of filter and catalysts used to treat the exhaust. These emissions such as NO_x , Particle Number (PN) and particulate matter (PM) from the engine are termed as 'local' emissions.

Over the years, as technology have been developed and the number of vehicles on the road have been increased, their emissions contributed to the rise in GHGs (global emissions) and air pollution (local emissions). This prompted governments to impose strict emissions legislation and testing procedures for vehicles in a move to curb these global and local emissions. By passing these regulations with laboratory testing only with standard driving cycles may lead to falsified conclusions, thus prompting for more real traffic scenarios. This is because there is a difference in inputs between a standard driving cycle (such as NEDC, WLTP etc.) and a real driving cycle, which is recorded by driving in real traffic. Such cycles can bring actual on-road behaviours in a laboratory test which was not possible with the standard tests. This led to the formulation of Real Driving Emissions or RDE tests that conduct emissions testings using portable measuring equipment to record real driving scenarios. This test was piloted in 2015 for EURO 6c as an additional but non-compulsive measure and is now made mandatory from EURO 6d-temp [1]. This is further discussed in Section 2.2.3.

Earlier, when the danger posed by diesel particulates of CI engines was recognised and addressed, there were many technological strides in making filters that could prevent such particles from escaping into the environment. At that time the focus was not the same towards gasoline emissions as the particles emitted from these engines were much finer and assumed to be harmless. Over time with advancements in gasoline engines and research around these finer particles, studies linked such particles (below 23 nm) to adverse health effects [2]. The need for recognising and regulating particles of diameters below 23 nm increased as the past and current legislation only accounted for particles which are greater than 23 nm. The introduction of Gasoline Direct Injection (GDI) technology brought many upsides in terms of fuel consumption and overall efficiency of engines to name a few. But this advancement had a downside as well. As there was a the drastic increase in particle number. This is owed to the fact that there are shorter mixing or evaporating times before combustion that can lead to an increase in particles in the form of unburned fuel and lubricating oil. These unburned condensed hydrocarbons have small traces of Poly-cyclic aromatic hydrocarbons (PAHs) along with organic species from PM emissions of GDI engines that are highly reactive in photo-chemical smog chemistry [3][4]. This agglomeration with other compounds or dissociation into smaller compounds leads to an increase in the number of particles. These PAHs are also well known for their carcinogenicity and effect on human health [5][6].

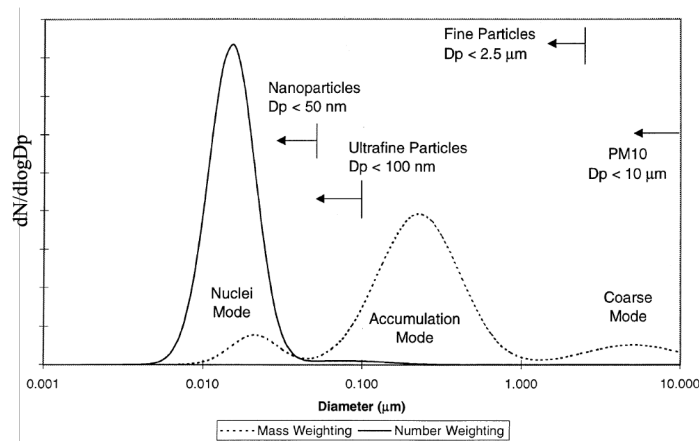


Figure 1.1: Typical engine exhaust size distribution both mass and number weightings are shown. (Image ref [7])

GDI engine exhaust particles are much finer compared to that of diesel soot, the majority being ultra-fine particles (UFP) (particle diameters $< 0.1 \mu\text{m}$) and fine particles (particle diameters $0.1 - 2.5 \mu\text{m}$). Figure 1.1 shows that most of the particle mass exists in the diameter range 0.1 to $0.3 \mu\text{m}$ called as the accumulation mode. Kittelson's [7] study describes that this is where the carbonaceous agglomerates and associated adsorbed materials reside. The diameter range 0.01 to $0.03 \mu\text{m}$ or the nuclei mode, usually consists of volatile organic and sulfur compounds that are formed during exhaust dilution and cooling, and may also contain solid carbon and metal compounds [7]. A study by Lenz et al. [8] explains that these GDI particles are much more reactive (i.e. oxidation and reduction) than diesel particulates. This is because of the low structural order of GDI particles compared to diesel soot. Further, nanotoxicology and epidemiological studies indicate that UFP have been hypothesized to have a direct impact on respiratory health conditions. Although there are few compelling epidemiological studies, toxicology studies do show interesting relations between UFP and adverse health issues [2][9]. The study by Chen et al. [2] cites sufficient evidence about how these UFPs impact human health as well as air pollution.

Real Driving Emissions have thus been introduced to explain the actual story of the gases emitted and their effect on the environment. The knowledge of the relationship between engine control and the EATS with several real driving conditions is still necessary to achieve lowered levels of local emissions. Hence, making investments in RDE research and development is all the more significant. In this study, the emissions behaviour of a typical gasoline PHEV are explored under real driving conditions and compare them with tests conducted on a dynamometer in a test-rig. This will also shed light on how the catalyst temperature, driving cycles, engine temperature, hybrid control strategy, ambient conditions and fuel affect the nature of PM emissions.

2 Background

The face of the automobile industry is fast evolving with the shift from ICE to hybrid vehicles and electric vehicles (EVs) as environmental problems become the cause of concern. Over the past years, the global sales of hybrid electric vehicles (HEVs) have been estimated to rise by almost 140% from 1.2 million in 2015 to 2.9 million in 2020 [InternationalAgency]. The European market alone has seen 900,000 units of HEVs being sold in 2018 which shows how the market is swiftly embracing this change. Furthermore, as this continues the impact on the environment grows leading to the search for new ways to curb the emissions and reduce well-to-wheel¹CO₂ for HEVs and EVs. The extent of reduction also depends on the power mix that is, CO₂ emission savings are significantly higher for electric cars used in countries where the power generation mix is dominated by low-carbon sources [InternationalAgency].

In countries where the electric power generation is dominated by coal and other high carbon sources, HEVs exhibit lower well-to-wheel CO₂ emissions than EVs [InternationalAgency]. Many countries offer benefits to buyers of HEVs and EVs in terms of reduced taxes and prices. This has aided the sales of these

¹A well-to-wheel analysis is an assessment of the environmental impact of a product or service throughout its lifespan.

vehicles and the global sales turnout exceeded 5.1 million in 2018, which is nearly doubling the new electric car sales from the previous year. Despite this shift, there are still a majority of cars with only ICE seen on roads and this will continue for the near future. Hence, the focus on treating exhaust emissions and the goal towards zero emissions remains a challenge. The PM emissions from a gasoline car mainly consist of hydrocarbons (HC), carbon monoxide (CO), soot, unburnt fuel and lubricating oil and oxides of nitrogen (nitric oxide (NO), nitrogen dioxide (NO₂)) collectively known as NO_x. The Figure 2.1 illustrates the compounds that have majority of the share in PM emissions from GDI engines. Current fuels like gasoline and diesel also contain minute traces of sulphur which is oxidised to produce sulphur dioxide (SO₂) [3].

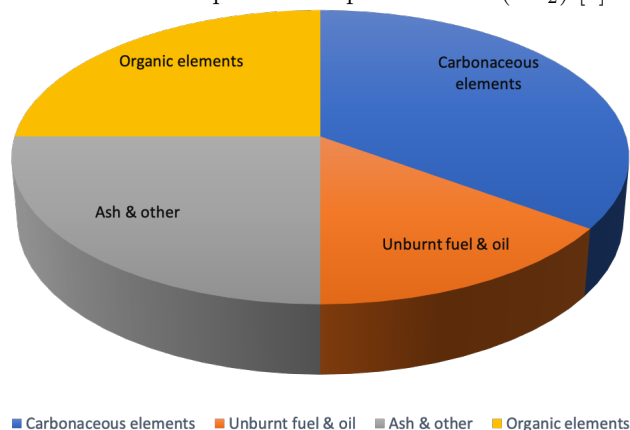


Figure 2.1: Typical PM composition of light duty vehicles with GDI engines (pie-chart distribution only for representation purpose. Image data ref [3])

NO_x is formed by the reaction of nitrogen and oxygen molecules during combustion, especially at high temperatures. It has significant repercussions on respiratory systems causing high levels of organ inflammation [10]. NO_x also contributes to the formation of ground-level ozone, which is also the cause of adverse health effects [3]. In areas of high motor vehicle traffic, such as in large cities, the number of nitrogen oxides emitted into the atmosphere as air pollution can be significant.

The direct fuel injection strategy for gasoline spark ignition engines injects precise amounts of fuel directly into the combustion chamber to mix with air supplied through the intake port. This fuel/air mixture is stratified or homogeneous ($\lambda = 1$) depending upon the need for power or fuel efficiency respectively. By keeping the mixture homogeneous, it benefits the three-way catalyst's (TWC) performance. A Three-Way Catalyst is a catalytic converter used to treat unburnt hydrocarbons (HC), carbon monoxides (CO) and oxides of nitrogen (NO_x) from the exhaust gases before being released into the environment. The TWC removes all three pollutants simultaneously by reducing NO_x to N₂, oxidising HC and CO to H₂O and CO₂ respectively. The catalyst's conversion efficiency is best when the air/fuel mixture of the exhaust is at or very close to stoichiometric value. The PM emission from the exhaust system can be filtered with the utilisation of a gasoline particulate filter (GPF). Based on the same functionality as a diesel particulate filter, it traps the ultra-fine particles from the GDI engine with the help of a filtering medium. The much lower PM emissions from GDI engines compared to diesel engines lead to a longer GPF ash build-up time. The high porosity and a thinner layer of ash also lowers the particle filtration efficiency of the GPF [11]. Hence, this filter needs to collect an initial amount of ash to reach a high degree of filtration. The EATS comprises of a general combination of a TWC and GPF in most modern gasoline and hybrid electric vehicles. This combination can be varied according to car manufacturers and government legislation. Their operating efficiency is a contributing factor that mandates the emissions of a vehicle.

There is a pressing need for cleaner and more efficient fuels in the transportation sectors as the worldwide resources of fossil fuels deplete at a rapid rate. The response of the automotive industry has been streamlined to these concerns since the last decade with the increased practice of blending gasoline and diesel with alternative fuels such as ethanol, methanol, natural gas (NG), bio-diesel and more. As described the greenhouse gas (GHG) emissions from vehicles are the significant contributors to global warming and climate change, a method called

Life Cycle Assessment (LCA) is used to evaluate the well-to-wheel greenhouse gas emissions of alternative fuels. Ou and Zhang (2013) [12] found that LNG-powered vehicles emitted 10 – 20% and 5 – 10% less GHGs than gasoline-fueled and diesel-fueled vehicles respectively. According to Yisong Chen et al.,2018 [13] NG mixed fuels have a higher brake thermal efficiency with low HC, CO and PM emissions than NO_x emissions.

On the other hand, the mixing of ethanol and methanol with gasoline for SI engine applications lead to a considerable reduction in HC, NO_x and CO emissions. The lower heating value (LHV) of ethanol and methanol is lower than that of gasoline, thus allowing for better and faster combustion through quicker evaporation, thus contributing to GHGs from increased CO₂ [14]. To minimise the adverse effects on vehicle emissions at higher levels of ethanol use, the engine and emissions control systems must be optimized for the fuel blend used.

2.1 Emission Standards

2.1.1 European Emission Standards

European emission standards are the exhaust emissions limitation standards for new motor vehicles which are being sold in the European Union and European Economic Area member countries. The European emission regulations for the exhaust emissions have divided motor vehicles into categories such as passenger cars, trucks, and off-road machinery depending on its bodywork, load as well as ignition type of particular vehicle model. For each vehicle categories, the different level of acceptable emissions is applied individually and the vehicle is assessed with standard test procedure in order to meet regulation compliance. In European countries, the exhaust emissions from motor vehicles are controlled by Low Emission Zone (LEZ) programs (or called Environmental Zones Program in Sweden), which are conducted either at country or local level, in order to meet EU Air Quality Standards [15]. Almost 30 years since the introduction of EURO 1 in 1992 until present, the regulations have become more stringent. Comparing the emissions limitation in Table 2.1 from EURO 5 to EURO 6, the allowance on PM is tighter and the PN limitation has been implemented. With this stringent regulation, it drives automotive manufacturers to take big strides in vehicle and engine technology development.

EURO 6 is the most recent emission standard for passenger cars by the European Union Commission. The standard is applied to both Gasoline and Diesel engine passenger cars and light commercial vehicles. Table 2.1 shows the various emission standards for gasoline passenger cars. The limitations of emissions level in each EURO 6 division are on the same level but an additional test procedure requirement has been regulated later in EURO 6c division for the RDE test. With this EURO 6 regulation, the light-duty vehicles are tested with an updated standard driving cycle from New European Driving Cycle (NEDC) to World Harmonised Light Vehicles Test Cycle (WLTC). Since, NEDC does not represent real driving behaviours and WLTC provides more dynamic driving behaviours. These cycles are further explained in Section 2.2.

Table 2.1: EURO Emission standards for Gasoline Passenger Cars [DELPHIPassengerVehicles]

Tier	EURO 1	EURO 3	EURO 5a	EURO 5b	EURO 6b	EURO 6c	EURO 6d-temp	EURO 6d
Type Approval Date	Jul-1992	Jan-2000	Sep-2009	Jan-2014	Sep-2014	-	Sep-2017	Jan-2020
First Registration Date	Jan-1993	Jan-2001	Jan-2006	Sep-2015	Sep-2015	Sep-2018	-	Jan-2021
THC [mg/km]	-	200	100	100	100	100	100	100
NMHC [mg/km]	-	-	68	68	68	68	68	68
HC + NO _x [mg/km]	970	-	-	-	-	-	-	-
NO _x [mg/km]	-	150	60	60	60	60	60	60
CO [mg/km]	2720	2300	1000	1000	1000	1000	1000	1000
PM [mg/km]	-	-	-	-	4.5	4.5	4.5	4.5
PN [# /km]	-	-	-	-	6×10^{11}	6×10^{11}	6×10^{11}	6×10^{11}
Conformity Factor	-	-	-	-	-	PN: 1.5	NO _x : 2.1 PN: 1.5	NO _x : 1.43 PN: 1.5
Test Cycle	Urban + Extra Urban Driving Cycle	NEDC	NEDC	NEDC	NEDC	WLTC, RDE	WLTC, RDE	WLTC, RDE

In supplement to the laboratory test, the requirement for an RDE test with conformity factors has been introduced for emissions allowance since EURO 6c. Since, the RDE test is carried out with a PEMS in outdoor ambient conditions, where there will always be ambiguities. The accuracy of the measurement devices is not as precise as a controlled laboratory test. The conformity factors (CF) are defined as not-to-exceed (NTE) limits where the error margin is taken into account and it is calculated as in Equation 2.1 [16].

$$NTE_{pollutant} = CF_{pollutant} \times EURO6d_{limit} \quad (2.1)$$

The temporary version of EURO 6d (EURO 6d-temp), the $CF_{NO_x} = 1 + 1.1$ margin of NO_x and the $CF_{PN} = 1 + 0.5$ margin of PN. In which the margin represents the uncertainty of measurements [17]. This means that the vehicles can emit NO_x 2.1 times EURO 6 limit and 1.5 times of PN limit. For the final conformity factors of EURO 6d, the $CF_{NO_x} = 1 + 0.5$ margin of NO_x and the $CF_{PN} = 1 + 0.43$ margin of PN. For example, the limitation of PN of EURO 6d-temp is 6×10^{11} #/km. With the conformity factor of 1.5, the allowance of the PN is be able to go up to 9×10^{11} #/km. And the acceptable level of NO_x can be expanded up to 85.8 mg/km.

2.2 Emission Test Procedures

2.2.1 New European Driving Cycle (NEDC)

NEDC is a driving cycle which was introduced in 1996 for fuel consumption and emissions testing of European light-duty vehicles. The driving cycle is divided into two parts, the first part (Phase 1) simulates urban driving conditions and the second part (Phase 2) simulates extra urban driving conditions. The urban part is repeated four times and is followed by the extra-urban part. The total distance of the NEDC is approximately 11 km with a duration of 1180 seconds and an average speed of 33.6 km/h [15].

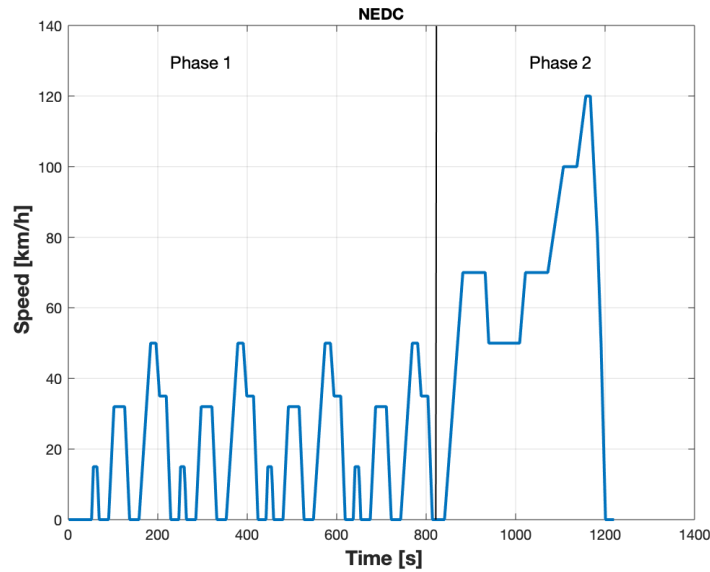


Figure 2.2: *NEDC Speed Profile*

Figure 2.2 shows the driving profile of NEDC in which the urban driving segment is very long, and the highway segment is short compared to city driving as well as accelerations are low and smooth. Moreover, the auxiliary devices in the vehicle are also not counted. These do not represent real driving conditions which contain several driving dynamics that have effects on fuel consumption and emissions. Furthermore, many new automotive technologies have been developed ever since then to reduce emissions. Today, the NEDC is considered to be out-of-date, since it has been used for over a decade and is no longer a valid cycle to justify the emission regulations for car manufacturers laid down by governments.

2.2.2 World Harmonised Light Vehicles Test Procedure (WLTP)

WLTP has replaced the NEDC since 2017. It was developed by using real-driving data from around the world to resemble realistic conditions. It was aimed to be applicable to vehicles worldwide so that the CO₂ emissions, pollutants and fuel consumption would be compared worldwide. It covers all traffic condition from urban to highway with sections involving accelerations, stops and braking phases. In the WLTP, vehicles are categorically tested with various cycles called as Worldwide harmonized Light vehicles Test Cycles (WLTC). These cycles are classified into three classes based on a power-to-mass ratio (PMR)² [15].

²The PMR of the test vehicle used for this study is 85 W/kg. This falls under 'class 3' of the WLTC cycles. The detail will not be gone through, since, it is not the main focus in this thesis.

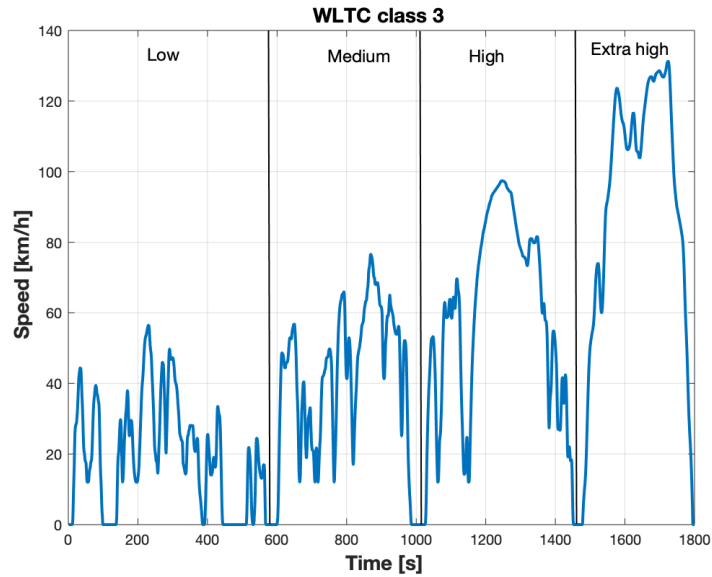


Figure 2.3: *WLTC Class 3 Speed Profile*

The WLTC Class 3 is broken down into two groups. The first group is 'Class 3a' whose maximum speed is less than 120 km/h and the second group is 'Class 3b' whose maximum speed is equal or greater than 120 km/h. The cycle is divided into four sections namely, low, medium, high and extra high based on the average speed and acceleration [15]. The WLTC is very dynamic and can be adjusted to test various kinds of vehicle powertrains such as conventional ICE, mild hybrid, PHEV and BEV. It also incorporates stricter car set-up and measuring conditions, thus being a better choice over NEDC.

2.2.3 Real Driving Emissions (RDE)

The real driving emissions test procedure is an additional test apart from the laboratory WLTP test for European emission regulations from EURO 6c onwards as a monitoring test for NO_x and a RDE test for PN with application of CF [DELPHIPassengerVehicles]. And the RDE test has been a mandatory test for regulation compliance, since EURO 6d-temp was introduced. It was developed to incorporate with the extent of driving in real-life conditions, hence, the name *Real Driving*. The RDE test is an on-road test procedure which is conducted on public roads with the utilisation of the PEMS. With this driving procedure, the test has a wider range of parameters and be able to cover a broad spectrum of driving scenarios and behaviours which are not incorporated in NEDC or WLTC.

A standard RDE trip consists of urban, rural, and motorway sections of the driving cycle. These sections are distinguished by speed limits that are set based on the testing party with further boundary conditions requirements mentioned in Table 2.2. For comparison purpose, driving conditions on each of the urban, rural, and motorway sections should be equally distributed within 10% tolerance in the relative distance. All in all, the total trip duration should last approximately 90 to 120 minutes [1] [16].

Table 2.2: Real Driving Emissions trip requirements [16]

RDE Requirements	Urban	Rural	Motorway
Vehicle speed (km/h)	0-60	60-90	>90 (>100km/h for at least 5 mins)
Distance (rel)	34% ($\pm 10\%$)	33% ($\pm 10\%$)	34% ($\pm 10\%$)
Min distance (km)	16	16	16

In addition to the RDE trip requirements, other boundary conditions shown in Table 2.3 such as ambient temperature, stop times, maximum speed, and altitude should be taken into account to fulfill test requirements and normalize trip configurations. The dynamic boundary conditions have been added to RDE legislative package to determine if the driving behaviors that could be too aggressive or too smooth.

Table 2.3: RDE Boundary Conditions [16]

Parameter		Provision set in the legal text
Payload		Less than 90% of vehicle weight
Altitude	Moderate	$\leq 700\text{m}$
	Extended	$> 700\text{m}$ and $< 1300\text{m}$
Altitude difference		No more than a 100-m-altitude difference between start and finish
Cumulative altitude gain		1200m/100km
Ambient temperature	Moderated	0°C to 30°C
	Extended	From -7°C to 0°C and 30°C to 35°C
Stop percentage		Between 6% and 30% of urban time
Maximum speed		145 km/h (160km/h for 3% of motorway driving time)
Dynamic boundary conditions	Maximum metric	95th percentile of $v*a$ (speed*positive acceleration)
	Minimum metric	RPA (relative positive acceleration)
Use of auxiliary systems		Free to use as in real life (operation not recorded)

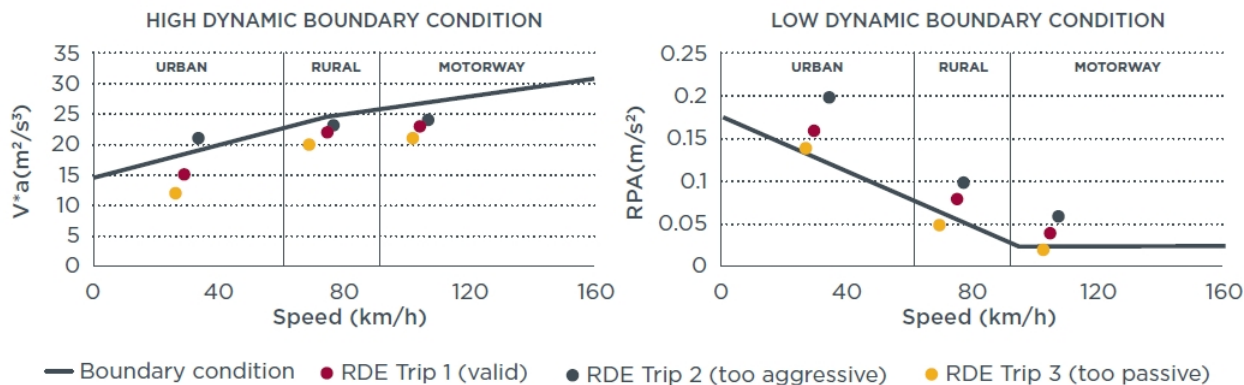


Figure 2.4: *Dynamic boundary conditions with three illustrative RDE trips [16]*

In order to validate the RDE trip, each urban, rural, and highway section should meet high dynamic boundary condition as well as low dynamic condition. In Figure 2.4 shows high and low dynamic boundary condition. For high dynamic condition, all driving sections must be under the line which represents speed multiplied by positive acceleration. For low dynamic boundary condition, all driving paths must be above the line which represents relative positive acceleration (RPA). These upper and lower limits are defined accordingly to Appendix 7a, section 4 of RDE 3 [1]. If the speed multiplied by positive acceleration is higher than the indicated line, the trip is considered being too aggressive and it's result is invalid. If the RPA is less than the indicated line, the trip is considered invalid as it is too passive or smooth [16].

3 Methodology

This chapter will provide a bird’s-eye view of every instrument, connection and data transfer of measurement process when a test is being conducted. This includes tests carried out in the test cell as well as on-road. Instruments such as the PEMS unit, DMS500, exhaust flow meter (EFM), GPS, and ambient sensors along with ECU data are used to record and collect data which is illustrated in Figure 3.1. All measured data from PEMS and ECU are received by the integration of AVL M.O.V.E System Control and ETAS INCA software, where they are recorded. Then, the recorded tests are post-processed by using AVL’s Concerto application. This recognises the signals and process time alignment between ECU and PEMS. And the software allows for viewing and exporting the signals. The RDE test results are obtained from here which is then used for analysis and reporting.

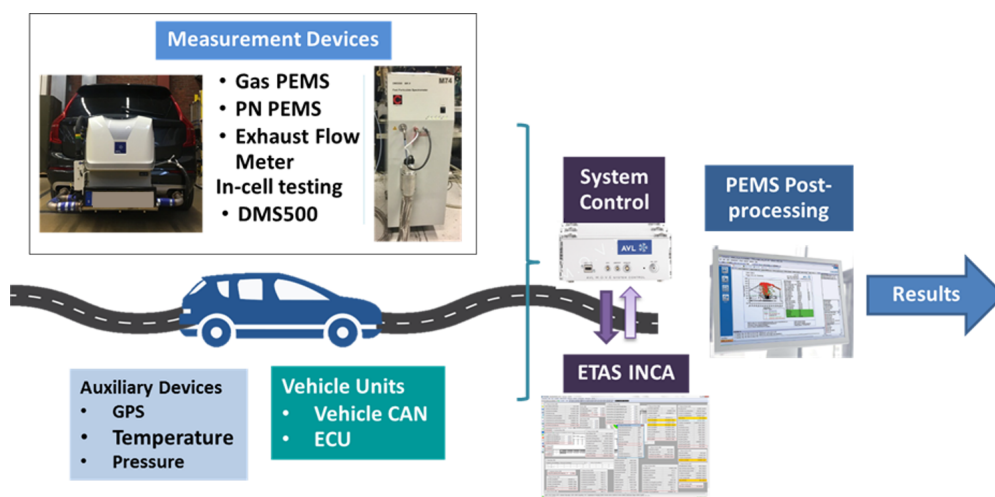


Figure 3.1: Flowchart of data and instruments involved in performing a complete RDE test.

3.1 Test Vehicle

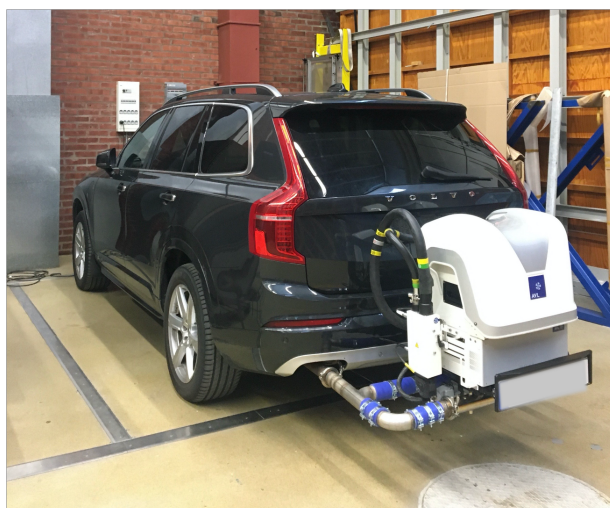


Figure 3.2: Test vehicle with PEMS mounted on the rear

The vehicle used in this study is a Volvo XC90 T8 2017 model year for sale in the European market. It is a gasoline plug-in hybrid vehicle with a 2L Inline 4-cylinder gasoline direct injection engine and an electric rear axle drive for electric propulsion through a lithium-ion battery. The hybrid engine is coupled with a crankshaft integrated starter-generator motor that is used to start the engine and also helps it recover otherwise

lost energy during slowing down ,hence the name 'Twin engine'. The EATS of this variant comprises of a coated GPF (TWC coated on the surface) and a TWC. The vehicle was previously modified for research and testing. Hence, the engine calibration nor the hardware can be considered to represent a normal production car. However, efforts were made to resemble the test vehicle to be as a production type vehicle so the results would be comparable. Furthermore, as the test vehicle is a 2017 model year and first registered in February 2016, it should be noted that the vehicle is registered with EURO 6b emission standard which does not require the vehicle to be tested with WLTP nor RDE according to EU registration number (EC) 715/2007 and (EC) 692/2008 [18] [COMMISSION6].

Table 3.1: Vehicle Specifications [VolvoTechnology]

Parameter	Unit	Description
Engine	-	T8 twin engine
No. of cylinders		4
Displacement	dm^3	2
ICE max power	kW	298 @ 5700 rpm
ICE max torque	Nm	400 @ 2200-5400 rpm
Electric motor max power	kW	87
Electric motor max torque	Nm	240
Battery capacity	kWh	10.4
Exhaust aftertreatment		TWC, Coated GPF
Fuel used		E85 ³
Model Year		2017
Production year		2016
Registration year		Feb-2016
Emission standard		Euro 6b
Driven mileage	km	4399

3.2 Portable Emissions Measurement System (PEMS)

The main measurement system in this study is the AVL PEMS unit as shown in Figure 3.2. The system consists of 'AVL Gas PEMS iS' and 'AVL PN PEMS iS' unit which are housed together on a supporting frame having restraints and also a license plate holder. The Gas PEMS analyses the exhaust gases and their characteristics whilst the PN PEMS measures the particle concentration of the exhaust gases. It comprises of auxiliary units like the calibration unit (eCAL), charging device, E-box (for mobile operation), batteries, heated sampling lines, GPS, Exhaust Flow Meter (EFM) and ambient sensors. These devices are connected to either the Gas PEMS and the PN PEMS unit through their respective ports to complete the full setup of the measurement system.

³A blend of 85% Ethanol & 15% Gasoline, RON 104



(a) PEMS mounted on towbar with its probe connected to the modified exhaust pipe



1 ... Power supply connection (POWER IN)
 2 ... On-Off switch (ON / OFF)
 3 ... Status LED (STATUS HEATING)
 4 ... Sample gas Inlet
 5 ... Electrical connection (heated) sampling line (SAMPLE LINE HEATING)
 6 ... Network connection (ETHERNET)
 7 ... Calibration connection (CALIBRATION UNIT)
 8 ... Drain outlet
 9 ... Maintenance flap
 10 ... Ventilation slide controls
 11 ... Main supply outputs (MAIN POWER OUT, MAX 30 A)
 12 ... Auxiliary supply outputs (AUX POWER OUT, MAX 10 A)
 13 ... Connection for power source/charging device (POWER IN)
 Attention: With no more than 30 A!
 14 ... Network connections (ETHERNET X1...X5)
 15 ... Indication of power source status
 Fig. 8

(b) Connection ports on Gas PEMS iS

Figure 3.3: PEMS connection ports and exhaust pipe modification

The PEMS unit has all the connections at the rear side of the device with connections for main power supply, Ethernet ports, sample gas inlet, calibration connection, drain outlet, maintenance flap, auxiliary supply and status LED as seen in Figure 3.3b. The Ethernet connections are made internally on the PEMS and also to an external PC which is capable of having remote access to 'AVL M.O.V.E system control' software on the PEMS. This remote access can also be wireless by establishing wireless link-up feature between the PC and the system control software. The electric power is supplied to the PEMS unit from the charging device to E-box through the attached batteries (mobile power supply) or from external power supply in test cell (stationary). These are the base unit which then provides electric power to the remaining connected units namely, the PN PEMS, eCAL, GPS, ambient sensor, heated sampling lines and EFM. Apart from the PEMS unit, the GPS and ambient sensor are mounted on the vehicle roof and remaining auxiliary devices are placed securely inside the vehicle and the wire and equipment arrangement are taken care of in order to prevent any leaks or electrical problems. An ingenious cover is built for the purpose of protecting the unit from weather and dust contamination as the local weather during the time of testing was rainy and cold (10 to 15°C) thus proving vital for testing. It covers the essential parts of the PEMS unit to prevent the external weather from having an effect on the measurement process as well as to prevent any damage on the measurement devices.

3.2.1 PEMS Working Principle

The PEMS unit is mounted on the vehicle tow bar and the twin-exhaust pipe is retrofitted with a modified pipe assembly as seen in Figure 3.3a to allow the PEMS unit and the EFM probes to be connected at the designated slots. This setup helps the PEMS unit to analyse the total released gases from both tailpipes. The EFM probes direct gases into the EFM to measure exhaust flow rate, exhaust pressure, and exhaust temperature. The sample gas inlet is connected to the VPR (Volatile particle remover) which dilutes the exhaust and removes volatile particles before the gas is sent to the PN PEMS. The gas for the GAS PEMS is sent unprocessed to the GAS PEMS through the VPR device and the eCAL box is used for calibration of the device before and after running tests. A leak check is performed by removing the gas from the system to see how well it can maintain vacuum pressure. While performing the tests it is important to have the drain hose directed downwards for easy flow of the gas and preventing any condensate formation inside it. This is imperious towards the safety and functioning of the equipment present inside the unit. The ventilation slides must be opened or closed depending on the atmospheric temperature being greater or lower than 10°C respectively.

To start the measurement, the AVL device control software is initialised to setup remote access with the PEMS unit which is established through the Ethernet port. The main operating device states of the PEMS unit are Standby, Hibernate, Pause, Switch on, Measurement, Purging, Leak check and Power off.

3.2.2 Instrument Layout And Measurement Principle Inside PEMS

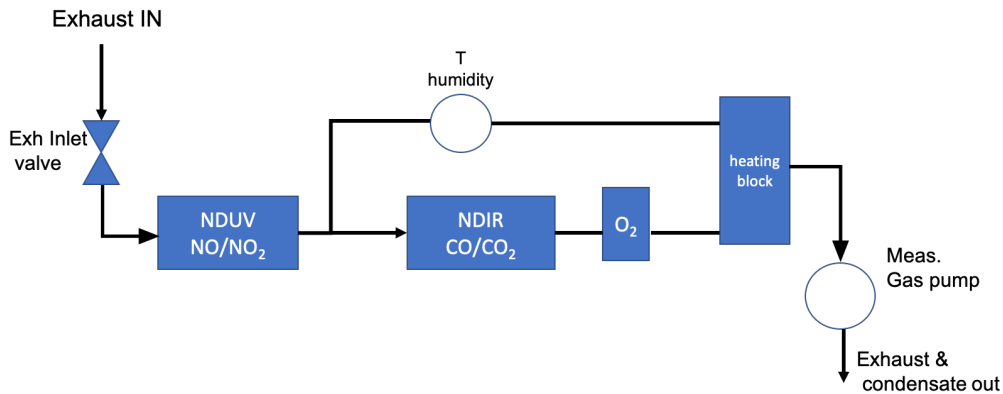


Figure 3.4: A simplified layout of measuring systems inside Gas PEMS

The probe from the exhaust pipe directs the gases into the PEMS measurement systems via the VPR. It is used to remove volatile particles and dilute the exhaust gases with cleaned hot air to a dilution ratio of 10. This mainly prevents any agglomerations or particle deposits from occurring inside the unit. From the VPR, the gases are fed to the Gas PEMS and the PN PEMS unit through heated sampling lines. These lines are heated to keep the gases from condensing within the pipe system and avoid damaging the internal parts and poisoning the measurement. In the Figure 3.4 a basic layout of the measuring instruments involved in the measuring process is shown. It should be noted that there are more instruments present in the actual layout but are not shown here as they are not of importance for this discussion.

The diluted gas that flows into the Gas PEMS unit is pre-cooled at ambient conditions and passed through a two-stage chiller. After the first chiller stage the gas passes through the NDUV analyser which measures NO and NO₂ separately. Downstream from here the gas is partially divided into two flows, one flow is directed to the NDIR analyser where CO and CO₂ are measured and the other flow is a bypass flow [19]. The oxygen is measured in the O₂ sensor and then the flows merge at the heating cum orifice block and then are pumped out via the drain outlet. The NDUV, NDIR and O₂ sensor measure pressure compensated concentrations in ppm or vol% [19].

Non-dispersive Ultraviolet Analyser (NDUV)

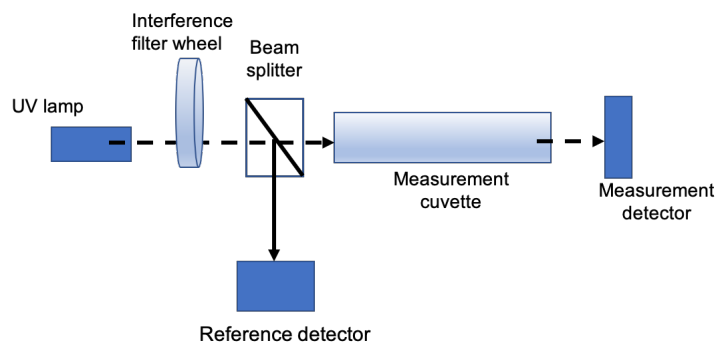


Figure 3.5: NDUV analyser measurement setup (Image ref [19])

This information is referenced from the AVL Gas PEMS iS product guide. The NDUV analyser is used to measure NO and NO₂ from the sample gas. The main components are the UV light source, measurement cuvette, reference detector, interference filter, beam splitter and a detector. The basic principle involves the UV radiation being absorbed by the molecules in discrete vibration absorption bands. This is then measured by the detector. The interference wheel is used as non-dispersive UV method to measure NO₂ and SO₂. The UV radiation emitted is split into a measuring beam and a reference beam in the beam splitter. This measuring

method is therefore a resonant method and is referred to as resonance absorption spectroscopy. The UV analyzer can be calibrated with internal calibration cuvettes which avoids carrying along an additional NO₂ calibration gas bottles on board the vehicle [19].

Non-dispersive Infrared Analyser (NDIR)

This information is referenced from the AVL Gas PEMS iS product guide. This NDIR analyzer is designed to obtain real-time concentration data for carbon dioxide and carbon monoxide from the exhaust gas stream supplied. It is specially optimized for a high accuracy and resolution of the CO channel at a measurement range below 0.1 vol% [19]. The main components of an NDIR sensor are an infrared lamp, sample chamber and a detector. The sample gas is made to pass through this chamber and subjected to infrared radiation by the lamp. This radiation is absorbed in specific wavelengths by the molecules according to the Beer-Lambert law which relates the attenuation of radiation to the respective molecule concentration. This attenuation of wavelengths is measured by the detector to determine the gas concentration. A filter presented before the detector eliminates any light other than the wavelength the gas molecules can absorb.

PN Sensing Unit

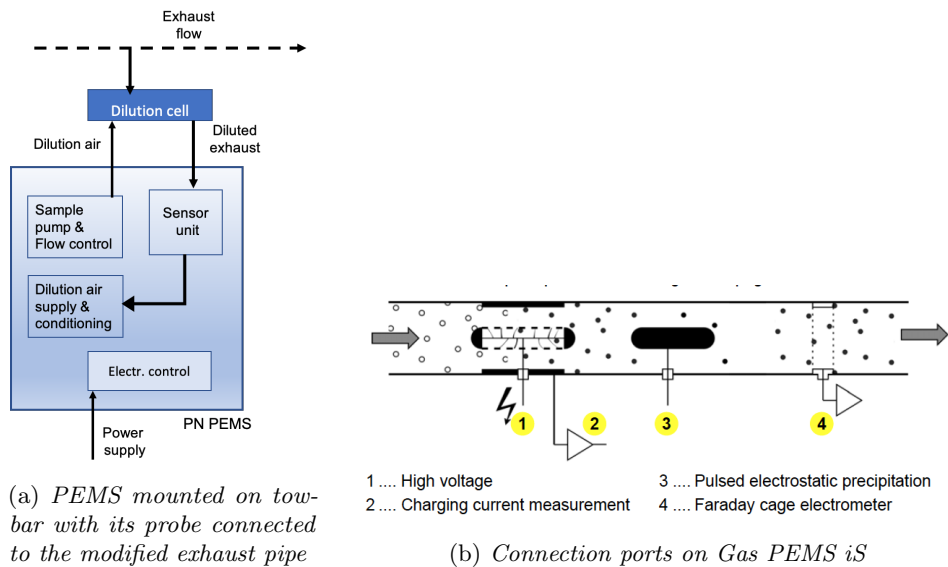


Figure 3.6: A simplified schematic of the components (Image ref [20])

This information is referenced from the AVL PN PEMS iS product guide. This sensor is presented in the 'AVL PN PEMS iS' unit of the PEMS unit. The diluted exhaust gas enters the sensor unit and is charged by a corona wire at high voltage. The gas particles are charged by the ions from the corona discharge by the method of diffusion charging (Figure 3.6b). This is followed by the pulsed electrostatic precipitator which produces a charge modulation in the gas. This modulation is then detected in the Faraday cage which is connected to an electrometer. So, every time a charged particle cloud passes through the Faraday cage a signal of compensated currents is detected, which is proportional to the charge of the particles. These signal peaks allow the sensor to calculate the amount of particles [20].

3.2.3 AVL M.O.V.E System Control

AVL M.O.V.E System Control is the name of the software is used with the PEMS unit. The System Control is a main control software for measurement devices, data acquisition and calculation of the results. It can integrate CAN bus signals from ETAS INCA to allow for result calculations. The System Control software also recognises additional measurement devices such as EFM, auxiliary sensors for ambient temperature, pressure, humidity and GPS apart from the PEMS unit.

During the main test, the emissions, driving conditions and ambient conditions are measured in real-time by the PEMS unit and recorded by the System Control software. It allows continuous monitoring of desirable signals during the test via a graph channel as in Figure 3.7. The RDE Testing Selection command can be prepared to set the application to determine vehicle speed ranges for urban, rural, or motorway mode. With this, while running the main test the window in Figure 3.8 will automatically pop up to display the status of numerous boundary conditions and show if they satisfy the RDE requirements for the test to be valid or not. When all the requirements are fulfilled, the measurement data will turn green which indicates the test is passed and valid for analysis. In the case of in-cell testing, the driving profile is provided to the test vehicle through a computer to actuators operating the pedals and the test vehicle is run on the dynamometer. For on-road testing, the RDE data is recorded using the System Control software and the test vehicle parameters such as engine speed, battery SoC level, vehicle speed, location of the vehicle and ambient conditions are measured by the communication of ECU, GPS, and auxiliary sensors. The CAN bus data such as, vehicle speed and engine speed is fed to the MOVE system control software which utilises these signals to compare the CAN vehicle speed data with the GPS vehicle speed signal and identify any discrepancies. They are also used in the calculation of several other parameters within the PEMS unit in order to provide useful final results once the data has been post-processed.

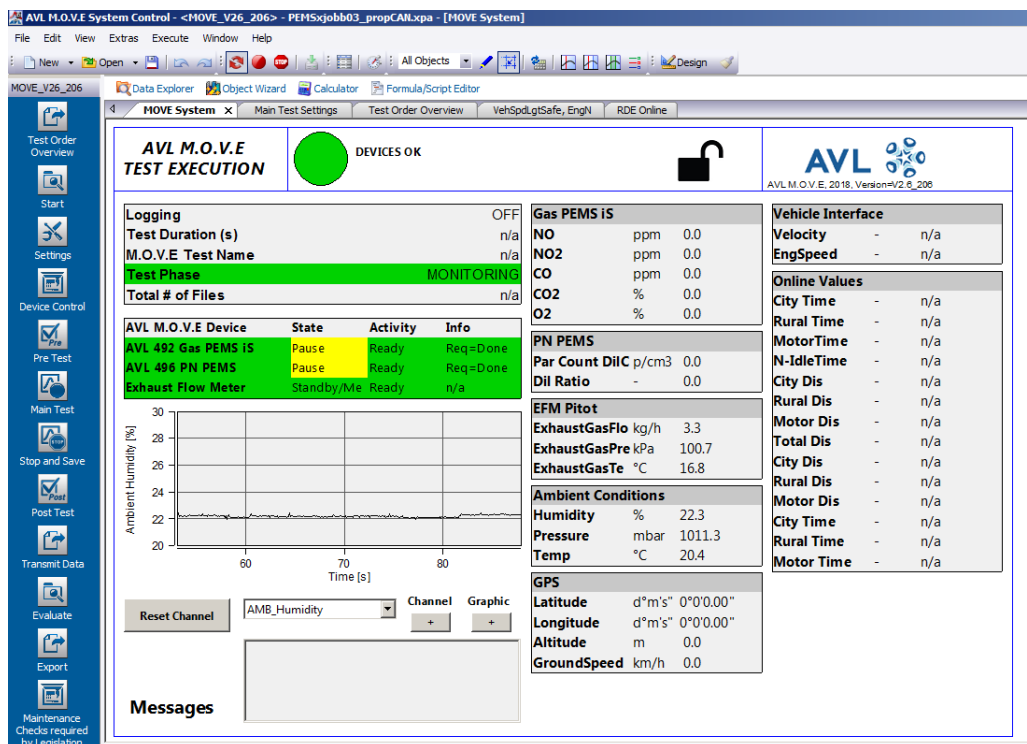


Figure 3.7: AVL M.O.V.E System Control Main Screen

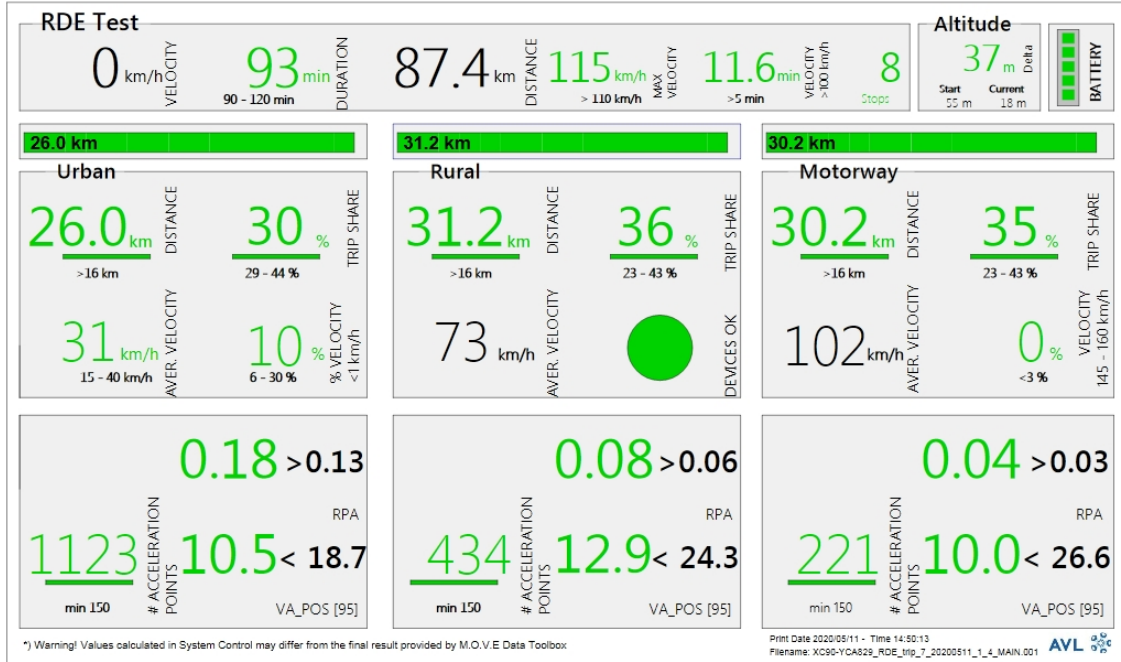


Figure 3.8: AVL M.O.V.E System Control: RDE Online Window

Emission Calculation

During the test, the exhaust emissions such as NO_x and PN are recorded in real-time resolution. They need to be calculated as a weighted average of the windows distance-specific emissions separately for urban, rural, and motorway categories [21] [22]. This calculation is done with a Moving Averaging Window method (MAW) where the test is divided into sub-sections or windows. This method allows identifying which windows are suitable to evaluate the vehicle RDE performance.

As the raw data of NO_x is measured in unit of ppm, it can be converted to grams for the distance specific emission calculation with exhaust mass calculation as following equations [22].

$$\text{Exhaust Mass Flow [kg/s]} = \text{Exhaust Volume Flow [m}^3/\text{s]} \times \rho_{exh} [\text{kg/m}^3] \quad (3.1)$$

The exhaust density can be calculated with standard pressure and temperature as Equation 3.2.

$$\rho_{exh} = \frac{P_{standard} \times MW_{exh} \times T_{standard}}{8314.15} \quad (3.2)$$

where MW_{exh} is Molecular Weight of exhaust gas [kg/kmol],

$$MW_{exh} = \frac{1}{100} \sum [44.01\text{CO}_2 + 32.00\text{O}_2 + 28.013\text{N}_2 + 18.015\text{H}_2\text{O}] \quad (3.3)$$

For EU legislation, the molecular weight of the exhaust gas is constant and is dependant on fuel type. Hence, the mass of pollutants is regulated by the calculation of the instantaneous mass emissions which is calculated as in Equation 3.4 with the value of u_{gas} for Ethanol in Table 3.2, in which, u_{gas} is a component specific factor or a ratio of density between densities of gas component and exhaust gas.

Table 3.2: Value of u_{gas} [-] in the raw and dilute exhaust gas for various exhaust components [22]

	NO_x	CO	THC/NMHC	CO_2	CH_4	Density
Exhaust raw	0.001587	0.000966	0.000479	0.001518	0.000553	1.2943
Exhaust dilute	0.001588	0.000967	0.000480	0.001519	0.000553	1.293

$$Pollutant [g/s] = pollutant [ppm] \times u_{gas} [kg/m^3] \times exhaust\ mass\ flow [g/s] \quad (3.4)$$

With this exhaust mass calculation. the mass of exhaust gas is divided by the weighting factor to distribute the emissions in each window.

$$M_{gas,d,k} [g] = \frac{\sum w_i M_{gas,d,i,j}}{\sum w_i} \quad (3.5)$$

where k = urban, rural, motorway, d = distance for each window, w = weighting factor for windows. i and j refer to time step and window respectively.

Then, the weighted distance-specific emissions for every category are calculated for the complete trip and each gaseous pollutant in g/km or #/km.

$$M_{gas,d,t} = f_u M_{gas,d,u} + f_r M_{gas,d,r} + f_m M_{gas,d,m} \quad (3.6)$$

where f_u , f_r , and f_m are 0.34, 0.33, and 0.33 respectively [22].

3.3 DMS500 Mk II Particle Analyser

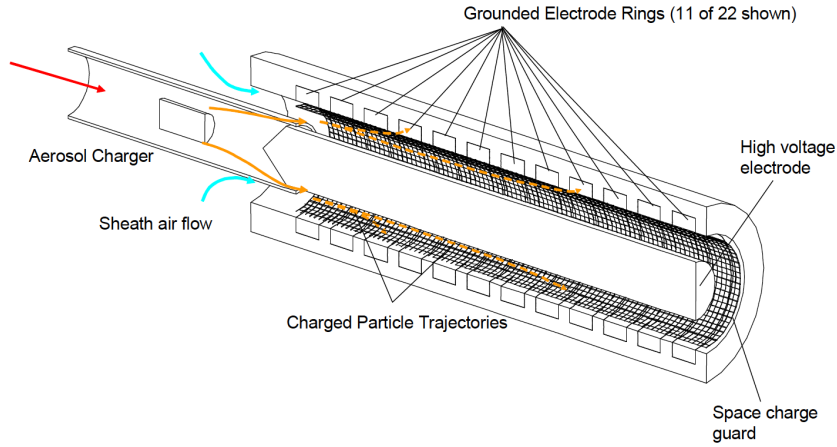


Figure 3.9: *Measurement operating principle of DMS 500 (Image ref. [23])*

This equipment is a real-time nanoparticle size spectrometer developed by Cambustion.Ltd. It is capable of measuring particle number, particle diameter (D_p) with size distributions from 5 nm to 1 μm [23]. It operates by directing incoming gases through a choked orifice into a classification section under high voltage discharge. The gas particles are charged proportionally to their surface area. They are introduced into an electric field with filtered sheath flow of air passing through it. The particles get attracted to the electrometer detectors and are detected at different distances depending on their aerodynamic drag and charge ratio. Based on this, the particle size and number are identified. Its data logging rate is chosen as 2 Hz with a very fast response to a concentration step change (T10-90%) of approximately 200 ms [23].

The DMS segregates the particle sizes into so-called 'bins' of data where each bin corresponds to a range of particle size. There are 38 such bins with particle sizes that vary from 4.87 to 1000 nm with logarithmically equidistant intervals. The DMS is not a highly portable device unlike the PEMS unit and hence is only limited to usage in test-cell testing. Henceforth, the data from the DMS will be directly compared with the tests from the test-cell only.

3.4 ETAS INCA

ETAS INCA is a calibration, measurement and diagnostic tool that allows the users to interpret data acquired by the engine control unit (ECU) with the help of the sensors. The software helps visualise data such as speed, temperature, torque, battery SoC level, voltage values and much more. It enables to instantaneously monitor the vehicle state during testing to make sure all necessary test conditions are met. All data that is recorded during a measurement is stored in a database. Multiple databases can be handled by INCA at the same time by its database manager GUI. ETAS INCA is used to record parameter signals from the powertrain and ECU, which are relevant for this study and cannot be obtained from the PEMS.

3.5 RDE Routes

The routes in this thesis are followed closely to the ones from the 2018 thesis by Ludvig Andersson and Mohammed Saeed [24], where the vehicle was driven on two routes; Landvetter (Figure 3.10a) and Kungsbacka (Figure 3.10b) in the Gothenburg region. Landvetter is a hilly road profile and Kungsbacka is a flat road profile. In the 2018 thesis, the routes were designed by considering RDE trip requirements and boundary conditions. Two different profiles were generated and validated by utilizing AVL software called RDE Route Identification application. The application generated the route by taking the RDE legislation into account and estimated the potential "RDE route" by considering traffic statistics such as speed limits, road closures and

other traffic conditions. Since this is 'real' driving, the speed profiles cannot be matched exactly to the routes from the 2018 thesis [24] but can be matched closely. Henceforth the term 'AMHN' will be used to refer to the 2018 Landvetter route and 'FLHC' will be used to refer to the 2018 Kungsbacka route used for test-cell testing. The terms 'Hilly' and 'Flat' will be used to refer to the 2020 Landvetter and Kungsbacka routes respectively.

Table 3.3: Route Specifications

Parameter		Hilly	Flat
Trip avg length		86.58	87.46
Cumulative altitude gain (m)		300	150
Altitude diff. between start and end point (m)		7	37
Trip share (%) km	Urban	27.2	29.7
	Rural	48.7	35.8
	Motorway	24.1	34.5
Trip avg duration (min)		98	93.5
Trip avg temp (°C)		14.15	10.8
Trip avg humidity (%)		40.43	31.22

The Landvetter (hilly) route begins at Chalmers and travels through Högsbo and Mölndal area of Gothenburg for urban part, then it continues to the rural part in Källered, Hällesåker and Härryda. The route continues on the motorway part on the Landvetter highway and then back into the city and ends at the start point.

The Kungsbacka (flat) route begins at Chalmers and passes through the city center of Gothenburg towards Frölunda. Then, it goes towards Särö and Kungsbacka for rural part and towards to Fjärås for motorway part and ends near Mölndal.

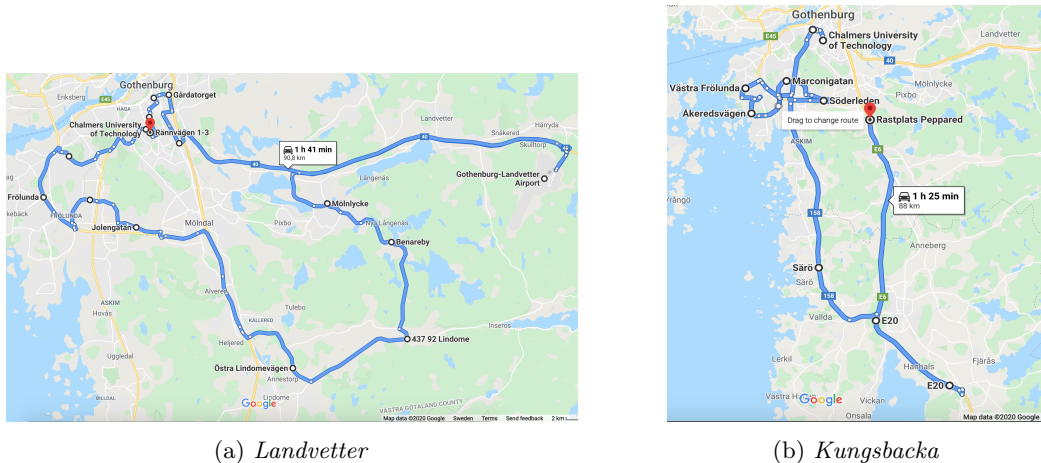


Figure 3.10: RDE test routes

4 RDE Experiment

This chapter will briefly go over the experiment procedure and the equipment required to perform an RDE test in test-cell and on-road.

4.1 In-cell Testing

In the test-cell at Chalmers, the vehicle equipped with the PEMS unit was mounted on the dynamometers of the test-cell. The mentioned driving cycles comprising data of vehicle speed (km/h), road gradient (%), and time (s) are simulated via the AVL PUMA system which is a test-cell testing setup. This driving cycle data is taken from 2018 thesis [24] raw data for the routes, Landvetter (Hilly) and Kungsbacka (Flat) respectively. Only driving cycles with hybrid driving mode and normal driver aggressiveness behaviour is chosen. The driving cycles and the RDE routes are explained in detail in Section 3.5.

The emissions were measured with the PEMS for every test and with the DMS500 in tandem for a few. Due to availability issues the DMS500 could not be used for more tests. Since, the PEMS only accounts for the number of particles and not their size, the DMS500 was used for this purpose. A setup of industrial fans used to simulate the wind at high speeds was made. This controlled setup compensated for the lacking aerodynamic resistance encountered at high vehicle speeds with the wind simulated for under-body airflow and front grille air intake for engine bay cooling. Another controlled parameter was the ambient temperature in test-cell which was maintained at 20 °C. The on-road test temperatures were at about 14 °C, which is below the minimum possible controlled temperature in the test cell.

4.2 On-road Testing

On-road testing had the PEMS mounted onto the tow bar of the vehicle with all connections and setup done to conduct the same test as in test-cell completely mobile. The internal battery power supply was used to provide electric power to PEMS and other devices during the trip. Once the pretest procedure was performed indoor, the vehicle is taken out on the chosen routes and trying to stay within RDE boundary conditions while driving around. The PEMS was protected from rain and dust with the cover made and once the trip came to an end the vehicle was brought into the indoor to perform the post-test check and the whole test was recorded. A total of four driving trips were recorded in this manner; two trips for the Landvetter (Hilly) route and two for the Kungsbacka (Flat) route. The vehicle was driven in hybrid mode with the battery SoC level between 18% - 22% in every trip. This was important for the comparison between the 2020 and 2018 studies. The on-road test temperatures were at about 14 °C, which is below the minimum possible controlled temperature in the test-cell.

5 Results and Discussions

This chapter will present the results obtained from all the tests performed and provide comparisons between the various combinations. These emission results will be discussed in-depth and reasonable explanations for their behaviour will be presented. To make it accessible for the reader to relate the discussions to the results, they will be presented in their respective subsections as follows.

5.1 Summary of results of all tests

Table 5.1: List of Testings For In-cell Testing and On-road Testing

Test Order	Test Name	Test Type	Measurement
Test 27	WLTC	In-cell	PEMS
Test 29	FLHC 1	In-cell	PEMS, DMS500
Test 30	AMHN	In-cell	PEMS, DMS500
Test 34	FLHC 2	In-cell	PEMS
Test 3.1	Hilly 1	On-road	PEMS
Test 3.2	Hilly 2	On-road	PEMS
Test 6	Flat 1	On-road	PEMS
Test 7	Flat 2	On-road	PEMS

The list of tests which were conducted both in-cell and on-road are shown in Table 5.1. The test order is nothing but the name given to the software and the test name represents the route. The emissions from in-cell testing and standard driving cycle; WLTC and on-road testing are presented in Table 5.2 and 5.3 respectively. For the in-cell testing, FLHC tests were done for two test orders. The FLHC 1 is the test which was performed with both PEMS and DMS500 units available for recording the emissions. However, this test was deemed inconclusive after it could not complete the whole drive cycle due to some technical issues with test-cell software. This resulted in the motorway section missing from the test. This test was performed once more later on where it managed to complete the full cycle but with only the PEMS unit for emission measurement. Tests on each RDE route have been performed twice. Figure 5.1 shows the speed profiles of FLHC and flat route and Figure 5.2 shows the speed profiles of AMHN and hilly route. Since RDE tests reflect the real driving conditions these figures are an explanation that for the designed route which was used for test-cell testing, the same could not be mimicked for on-road testing.

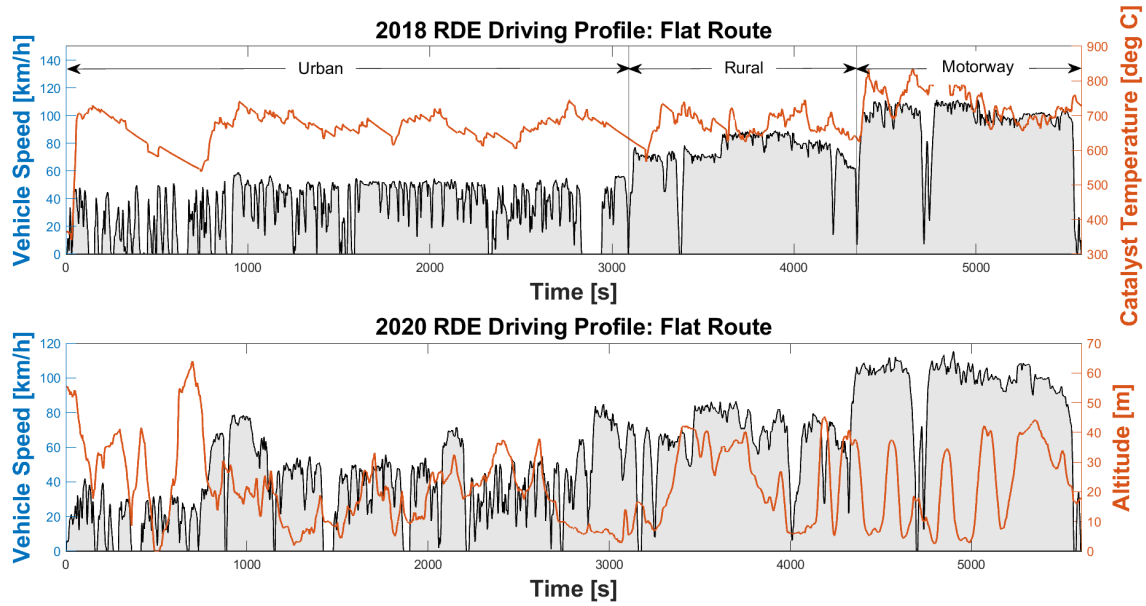


Figure 5.1: *Driving profiles of RDE Designed Flat Route (upper) & RDE 2020 Test Flat Route (lower)*

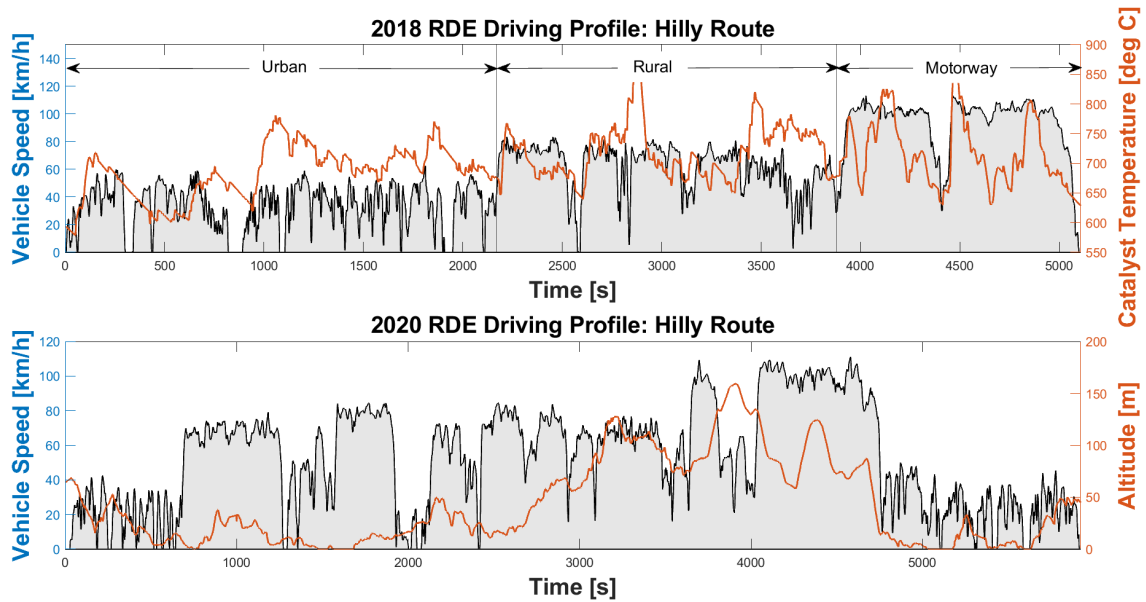


Figure 5.2: *Driving profiles of RDE Designed Hilly Route (upper) & RDE 2020 Test Hilly Route (lower)*

In Table 5.2, the WLTC is shown with a value of 1 as a scale factor for the emissions. This is done so the comparison with in-cell between on-road RDE tests to WLTC is easily understood with a normalised value of emissions. For example, if the PN of WLTC is 1 and the PN of AMHN is 1.51, it means that the AMHN has higher level of PN than the WLTC by 1.51 times. Referring to Table 5.2 and 5.3, the level of NO_x which is converted from raw data in ppm to g/km with the method of distance specific emission performed by the post-processing software. The NO_x levels of majority of the trips are negative except for Flat 1. This negative value implies that there is no NO_x emission from the test vehicle for that particular test. However, for the trips Flat 1 and WLTC which have a positive NO_x value, their levels are still considered as low. Comparing between test-cell and on-road testing, the NO_x levels from all tests are extremely low.

In order to have an easy and concrete comparison, the PN level in terms of #/km is calculated for all

tests which are utilised further for analysis and discussions. According to Tables 5.2 and 5.3, all RDE tests have a higher PN level being mostly 1.5 times higher than the WLTC. This can be due to the difference in engine-start operation in the driving cycle as the RDE has higher driving dynamic behaviour than the WLTC. Also another reason being that these RDE tests run for a longer period of time, almost 3 times as that of the WLTC. The total PN per trip for the on-road tests (Hilly 1,2 & Flat 1,2) is higher than those performed in the test-cell by approximately 15%, which used the driving cycle data from 2018 tests (AMHN and & FLHC-2¹). If considering the PN level for urban and rural section of the hilly trips, the level is much higher (almost 60%) than that of AMHN. The difference of total PN per trip between flat and FLHC tests is approximately 15%. And for the rural section it is roughly 18% - 29% and 32% - 36% for the motorway section. This is about half the hilly route.

Table 5.2: Emissions Summary for Test-cell RDE trips and Standard WLTC

Emission	Unit	AMHN	FLHC 2	WLTC
NO _x	-	-0.21	-0.09	1
NO _x Motorway	-	-4.98	-2.15	1
NO _x Rural	-	-8.69	-3.74	1
NO _x Urban	-	-0.08	-0.03	1
PN	-	1.51	1.45	1
PN Motorway	-	2.65	2.54	1
PN Rural	-	1.36	1.30	1
PN Urban	-	1.15	1.10	1
Trip Duration	s	5570	5890	1819
Trip Distance	km	86.20	85.65	23.15

Table 5.3: Emissions Summary for On-road RDE trips

Emission	Unit	Hilly 1	Hilly 2	Flat 1	Flat 2
NO _x	-	-0.36	-0.28	0.18	-0.23
NO _x Motorway	-	-8.69	-6.72	4.38	-5.51
NO _x Rural	-	-15.15	-11.72	7.63	-9.60
NO _x Urban	-	-0.14	-0.11	0.07	-0.09
PN	-	1.52	1.77	1.63	1.72
PN Motorway	-	2.67	3.10	2.86	3.01
PN Rural	-	1.37	1.59	1.46	1.54
PN Urban	-	1.16	1.35	1.24	1.31
Trip Duration	s	5924	6057	5974	5610
Trip Distance	km	86.58	86.5	86.52	87.46

¹FLHC-2 is a test-cell trip which completed the full cycle period. FLHC-1 otherwise called as simply FLHC throughout this study is the trip which was incomplete with the motorway section missing. This numbering aims to avoid further discrepancies

5.2 Standard Driving Cycle WLTC

Apart from the in-cell and on-road RDE testings, the standard driving cycle WLTC was also tested in test-cell to observe behaviour of NO_x and the PN. The results of the WLTC cycle will be discussed and analysed in this section. Since, this test was performed under the same conditions as those for other in-cell tests, the emission behaviour can be linked with that of RDE tests. In the previous section of result has mentioned that the overall level of exhaust emissions from WLTC was relatively low for NO_x and the total PN per trip of WLTC was lower than both of the in-cell RDE and on-road RDE testings.

In Figure 5.3, one can observe how the driving cycle does not demand for any support from the engine for the first 600 seconds. There after the engine is utilised on three separate occasions to support the power demand from the vehicle as the battery SoC reaches its lower limit (not shown in the figure). The engine charges the battery and propels the vehicle during this time until required. At the instance of first engine-start (618 s), it can be seen from Figure 5.3 that the PN rises instantly after a few seconds of delay (2 to 3 seconds which is the residence time for the gas in the system) as the catalyst is still cold (150°C) and needs to warm-up before it can reach its optimal conversion efficiency. This is also the reason for a spike in NO_x from 0 to 160 ppm (Figure 5.6) at this time. It can be seen that as the catalyst temperature rises after a few seconds the NO_x level subsequently lowers and then goes to zero. The cold start alone is not the reason for the increase in PN during engine-starts. It will later be shown how the PN behaves for every engine-start and what factors contribute to this behaviour.

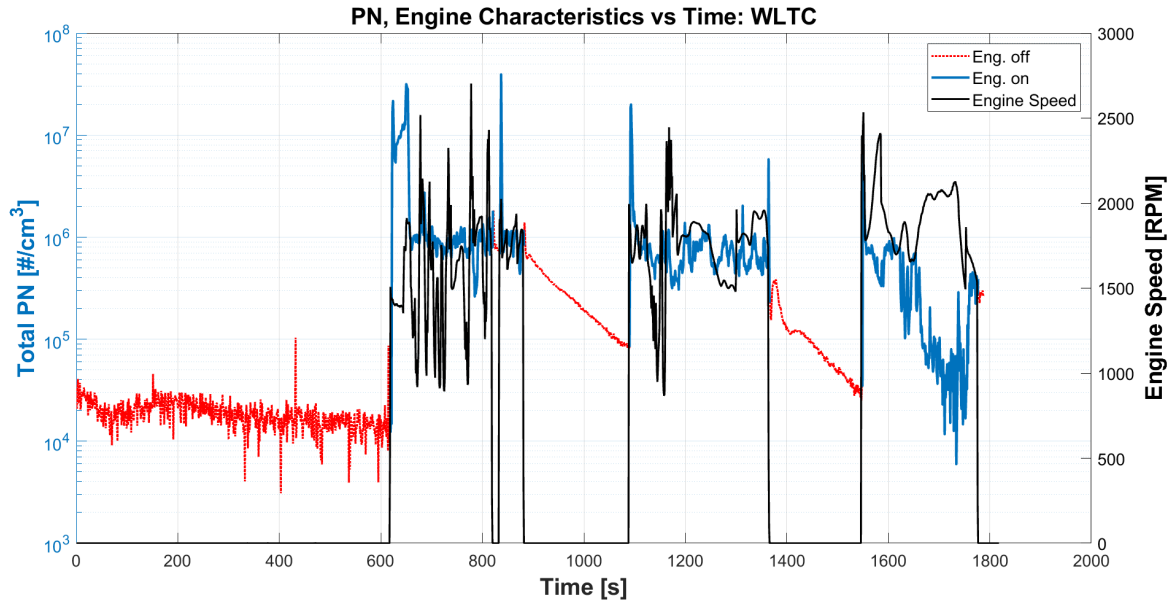


Figure 5.3: *Behaviour of PN with Engine and Vehicle Characteristics: WLTC*

Figure 5.4 shows the PN and engine speed and Figure 5.5 shows the PN along with fuel rate and fuel mass injected. The blue line in both figures represents the PN during the period of engine-on and the red dash line (Figure 5.5) represents the PN during engine-off. In WLTC, the period for which the engine is operated is shorter as the power demands from the cycle are not very extreme which would force frequent engine starts. So, the peaks of PN presented are subsequently lesser than in RDE trips. During this engine-start, after the PN reaches the peak level at the beginning, there is a trailing level of PN recorded until the engine is off. There is some "tail" at the beginning of engine-off period which is the residual of the particulate which has remained in the exhaust system and is still being released during this time. However, after a few seconds the PN level reaches zero.

A closer look at Figure 5.5 tells how the amount of fuel injected at the first engine start plays a contributing factor in the PN behaviour. Since the engine is "cold" the vaporization of the fuel injected is slow thus prompting higher fuel rate which can be seen at 618 s. This will create a temporary fuel-rich mixture.

Thus, until the engine warms up and the fuel enrichment stops more HC and CO emissions can be expected. This can also explain for the "tail" behaviour in the PN after the initial spike.

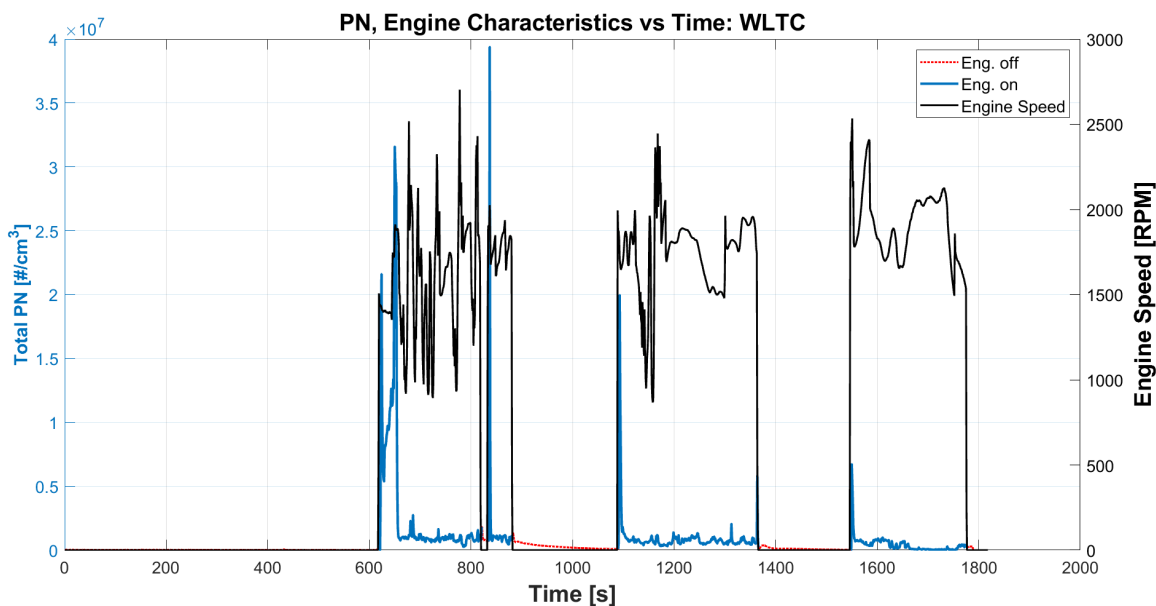


Figure 5.4: Behaviour of PN with Engine and Vehicle Characteristics: WLTC

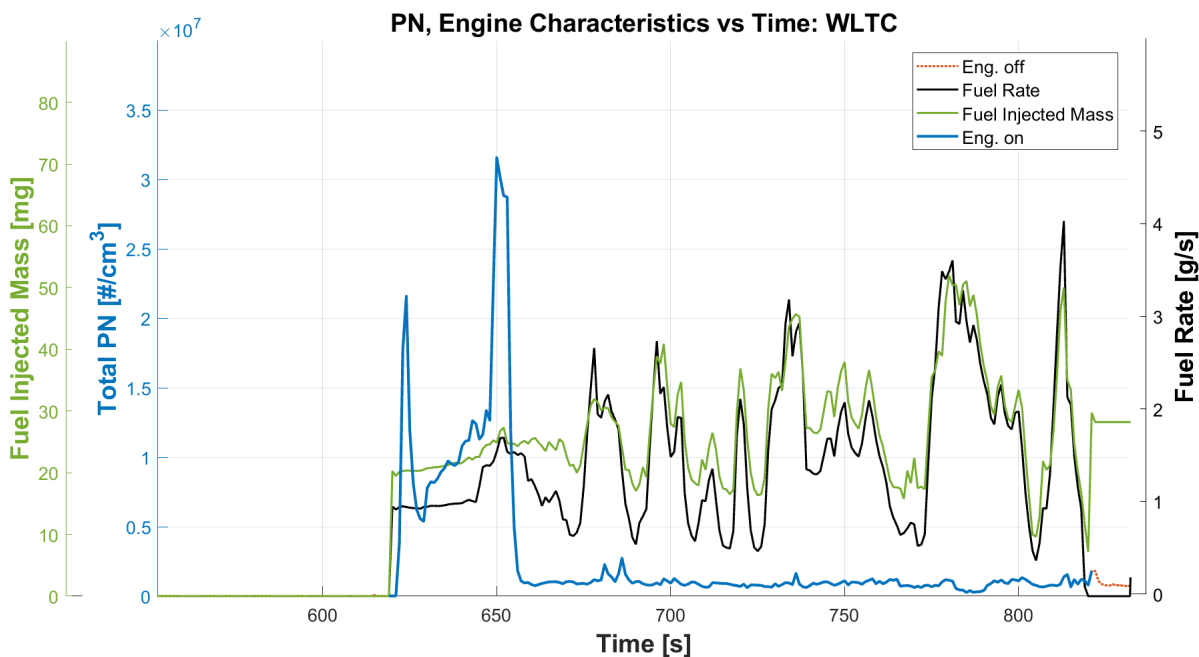


Figure 5.5: Behaviour of PN with Engine and Vehicle Characteristics: WLTC

In WLTC there are fewer spikes of NO_x and PN. The level of the NO_x peaks are relatively low, where, the highest peak is approximately 165 ppm and the low levels are between relatively 0 to 70 ppm. In WLTC, the cold start behaviour can be observed. At the beginning of the cycle, the catalyst temperature is approximately 150°C , thus making it a "cold" catalyst. Since, the engine does not start until 620 s, there is extremely low level (almost zero) of NO_x emitted from the engine during this time period. As soon as the engine is on the

NO_x abruptly rises up to 170 ppm. This behaviour can be explained by the engine's operation. As the engine has been off for 600 s the catalyst is not warm enough, so when the engine is on the catalyst is not warm enough to reduce NO_x . After the engine has been on for some time and the catalyst heats up, the NO_x reduces to a low level and even reaches zero after 800 s until the end of the cycle.

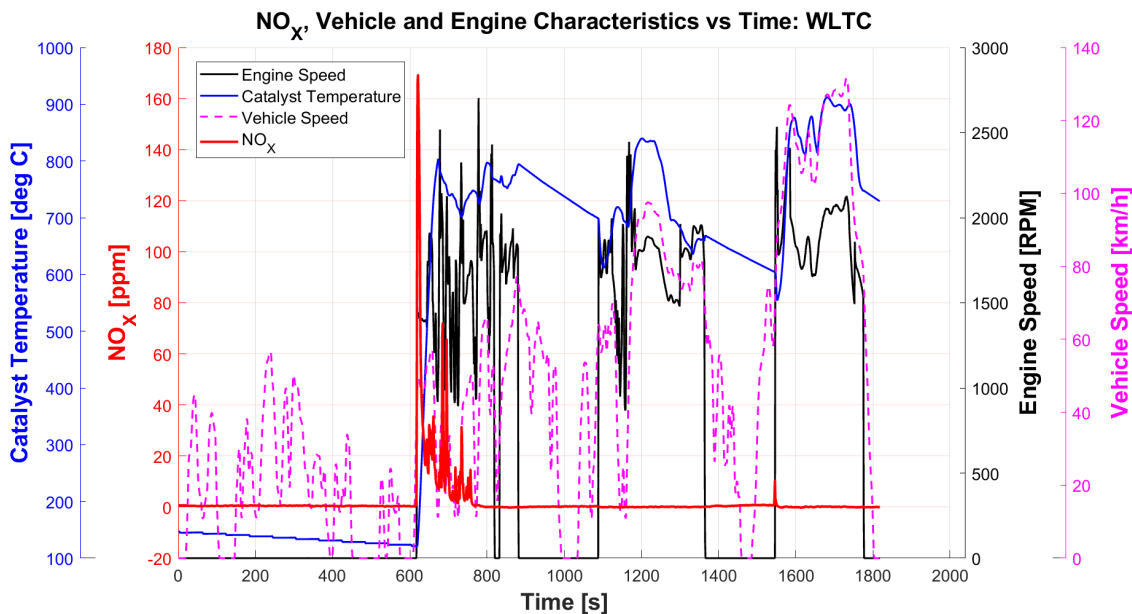


Figure 5.6: Behaviour of NO_x with Engine and Vehicle Characteristics: WLTC

5.3 RDE: NO_x

The behaviour of NO_x at tailpipe is seen in Figure 5.7 for both flat and hilly on-road RDE trips. It suggests that there is virtually no NO_x emitted when this is compared with standard tailpipe NO_x emissions from conventional ICE vehicles. The spikes in NO_x tend to appear at the beginning of the trips when the engine starts for the first time and the TWC is not warm enough to reach the desired filtration efficiency. Moreover, with the real traffic and road conditions, the test vehicle stopped frequently and this might cause the catalyst temperature to drop forcing more warm-up time. The trends of NO_x levels are mostly showing zero. Generally, gasoline engines do not produce much NO_x compared to diesel engines. This is because of the higher compression ratio in Diesel engines and this higher compression generates more heat and pressure which are the main reasons for NO_x formation. Since these tests were recorded with E85 as the fuel, this would further reduce the NO_x levels at engine-out and tailpipe.

When considering the NO_x peaks from Figure 5.7, the low level of NO_x for the Hilly 1 (22 ppm) as well as the peak of WLTC (170 ppm) should be considered as 'high' value compared to other trips whose levels are below 10 ppm or even close to zero. This would make the highest peak from WLTC (170 ppm) insignificant when looking at the cycle as a whole. Generally, for SI engines the amount of NO_x depends on the engine design and operating conditions with the typical amounts ranging from 500 to 1000 ppm [3]. Moreover, from the study of emission from SI engines with Ethanol blend with gasoline by Musaab O. El-Faroug et al. [25] it is found that at fixed engine speed 2500 rpm, at lean operation, the engine emits 1300 to 2100 ppm of NO. The exhaust temperature and ignition timing also play a role on NO and NO_x emission but normally at constant speed the level of NO_x is around 500 ppm to 2200 ppm. Hence, the value of the peak can still be considered as low level.

Another observation in Figure 5.7 is the CO level. The variation of CO does not depend on number of engine starts but the operation of the TWC along with the lambda sensor. The lambda sensor which usually sends feedback signals about the oxygen content in the exhaust emissions to the ECU, plays an important role in keeping the engine running stoichiometric. This is crucial for the TWC conversion efficiency. However, from

Figure 5.7 it is seen that although NO_x is very low CO level is high thus concluding that the TWC is not performing as it should. The speculation is that the lambda sensor is malfunction, making the engine run rich most of the time resulting in such low NO_x levels. Despite this dis-functionality the lambda sensor does not have any effects on PN emission and it is still be able to do an analysis.

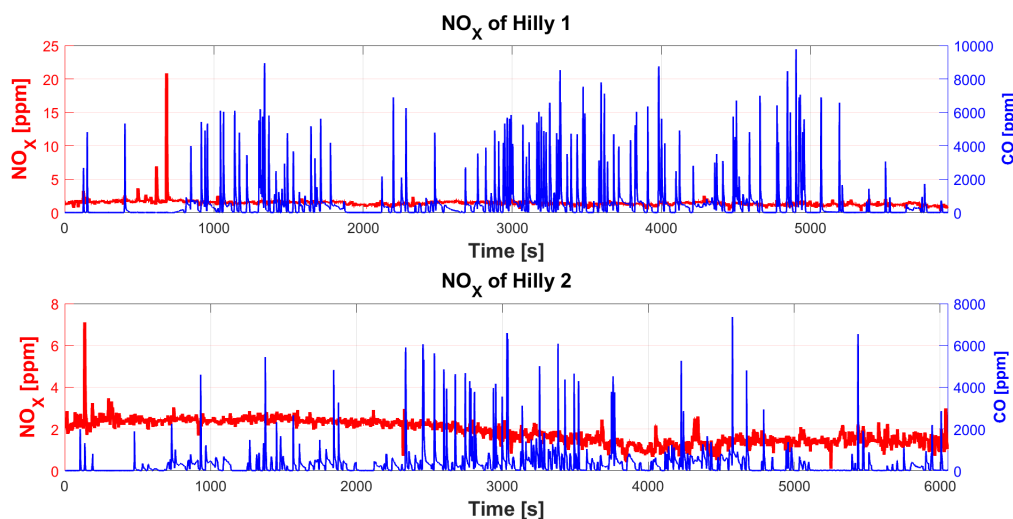


Figure 5.7: NO_x vs. Time: Hilly Route

In order to study more about the NO_x behaviour, following Figures 5.8 & 5.9 show a closer look at the peak along with fuel rate, catalyst temperature, engine speed, vehicle speed and crank torque. As mentioned before that the NO_x peak has a tendency of occur at the beginning of the trip. In Figure 5.8 the peak of NO_x of trip; Hilly 2, at the first couple minutes of the trip the catalyst temperature is around 525K to 600K, NO_x suddenly reaches the high point at 4 ppm. However, the behaviour of the catalyst temperature is different for trip; Hilly 1 as in Figure 5.9, where the temperature drops even if the engine is operated. However, the released NO_x is still an acceptable level. Moreover, if one observes at the relationship between engine switch on and off, it is noticeable that at the point where engine is off (engine speed is zero) the catalyst temperature slightly decreases. When engine is on, the catalyst warms up and its temperature rises. This phenomenon can be a result of the peak of the NO_x . Before the peak of the NO_x at 680 s in Figure 5.9, the engine had been on and off for couple of times and the engine-on period is shorter than the engine-off period which does not allow enough time for the catalyst temperature to sufficiently heat up. When the vehicle speeds up from urban to rural part, the NO_x abruptly surges. Then, the engine is continuously on the run and allows the catalyst to be heated up, the amount of NO_x is reduced. As the catalyst temperature also relates to the engine operation. This can affect the efficiency of the TWC.

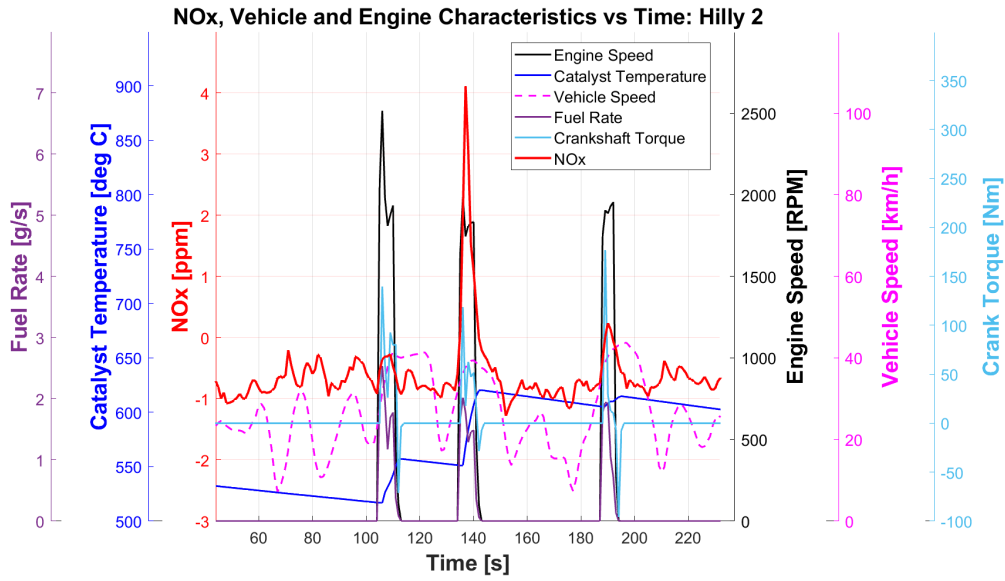


Figure 5.8: Behaviour of NO_X with Engine and Vehicle Characteristics: Hilly 2

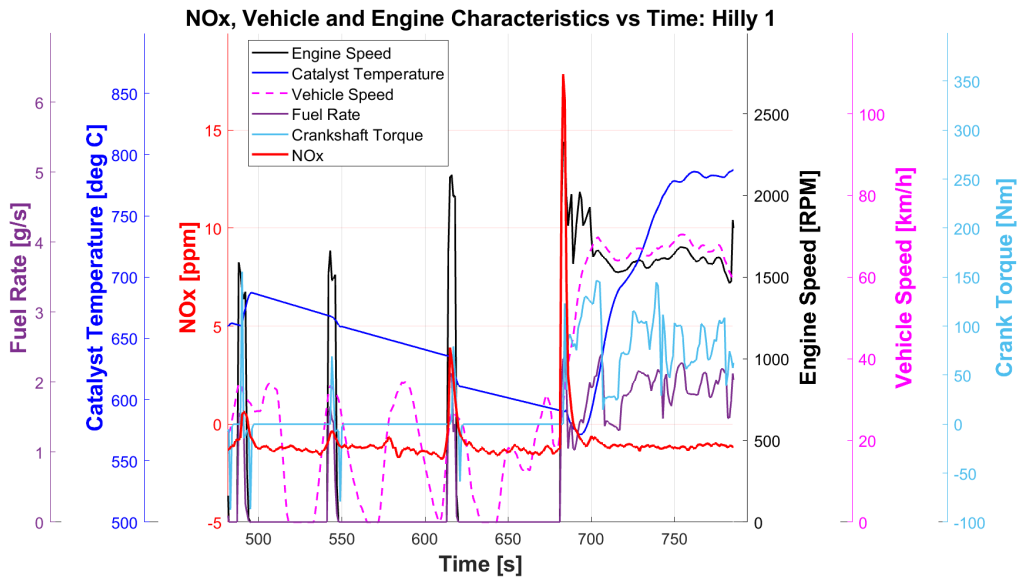


Figure 5.9: Behaviour of NO_X with Engine and Vehicle Characteristics: Hilly 1

5.4 RDE: Particle Number

Here the particle number behaviour associated with the on-road tests performed is studied closely. A comparison between the two measurement instruments is done to check their behaviour.

5.4.1 Behaviour of Particle Number

In this section, the behaviour of PN will be discussed. In Figure 5.10 the peaks of PN occur in every engine start as observed earlier in the WLTC cycle. The level of engine speed does not have an influence on the amount of PN that will be emitted.

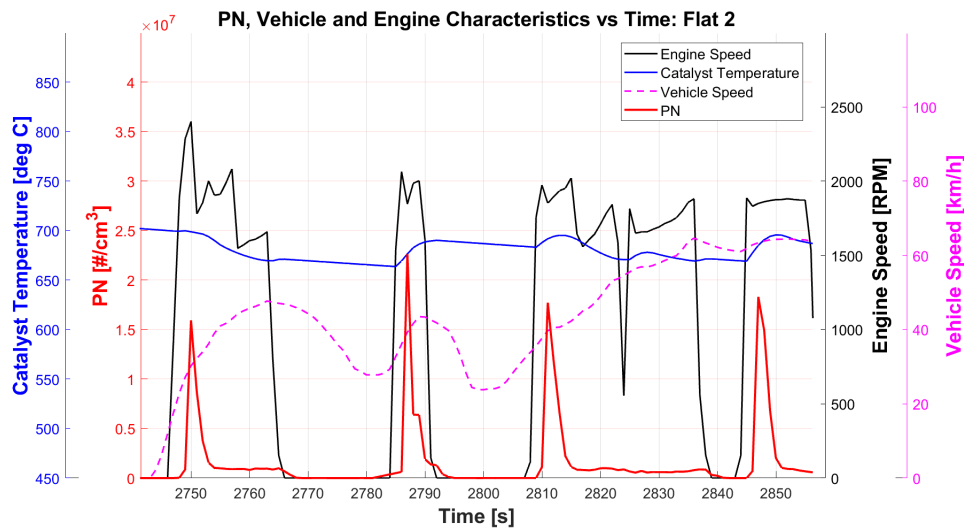


Figure 5.10: Behaviour of PN with Engine and Vehicle Characteristics: Flat 2

For example, comparing the level of PN peak during 2750 s with 2790 s, even though at 2790 s has higher engine speed but it has less PN than at 2750 s for almost half amount of it. Another observation is at the points where the engine has been operated for such a long period of time as at 2750 s to 2770 s and 2810 s to 2840 s, after the PN has reached the highest peak, there is still a "tail" of small level of PN left until the engine is off again. If this small tail behaviour is associated to each engine operation then long periods of operation can amount to high levels of PN.

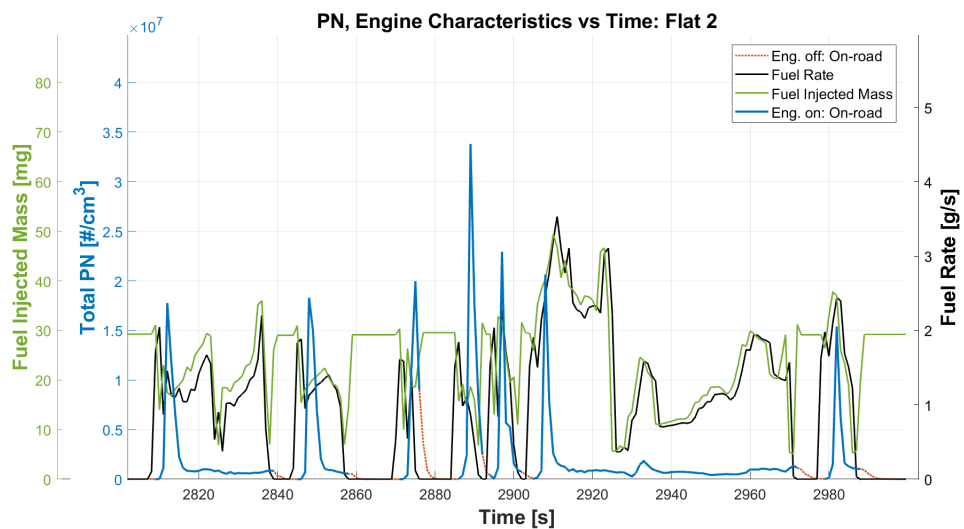


Figure 5.11: Behaviour of PN relative with fuel rate: Flat 2

Besides the effects of engine speed and catalyst temperature, fuel rate and mass of fuel injected has also played a role on the PN emission. In Figure 5.11, the peaks of PN fall after the initial amount of fuel is injected. This is because of the fuel enrichment. Moreover, as long as the fuel is injected, there is still some particulates being released. This also means that the whenever there is fuel in the engine, there will be particulates. Considering the relation between fuel rate and fuel injected mass, these two fuel characteristics are related to each other as well as engine speed. During such transient behaviour of the engine when the fuel is injected into the combustion chamber, there is a fraction of the fuel that quenches on the cylinder walls, the piston head and a fraction that escapes into the crevice between the cylinder head and the wall. All of these phenomena occurring if not simultaneously, contribute to the unburned HC during the expansion and exhaust

strokes of a combustion cycle. This unburned HC can further downstream lead to increase in particles as it can adsorb and desorb with other particulates from the exhaust [3]. Along with these, the bulk quenching of flame in that section where the engine speed is especially low also contributes to the unburned HC formation. Such conditions are very much plausible during transient engine operation when the fuel/ air ratio, spark timing and exhaust gas recycled from the emission control are not properly matched [3].

5.4.2 Comparison between PEMS and DMS500

The logged data from both the measuring instruments are carefully analysed and then compared with one another. To have a fair comparison, a few steps have to be taken before data analysis, since the instruments have different measuring capabilities. The data from the DMS500 is tailored to be in the same range as the PEMS which has a smaller particle size detection range (23 - 200nm). This is important as the total particle number count directly depends on the number of data bins taken into consideration from the DMS500. When parsing through the data-sets null values are observed at certain time points, which, can be regarded as measuring errors. These null points were interpolated using MATLAB without altering useful data for better result analysis, understanding, and allowing to make realistic conclusions. The Figure 5.12 illustrates the logged PN data comparison between the two instruments for AMHN cycle. In Figure 5.12 the plot lines overlap with minor inconsistencies revealing the error between the PEMS and DMS500. This is the Landvetter (hilly) route mentioned earlier in section 3.5 which is performed in the test-cell. Since, there were no disruptions during this test run, good data was obtained.

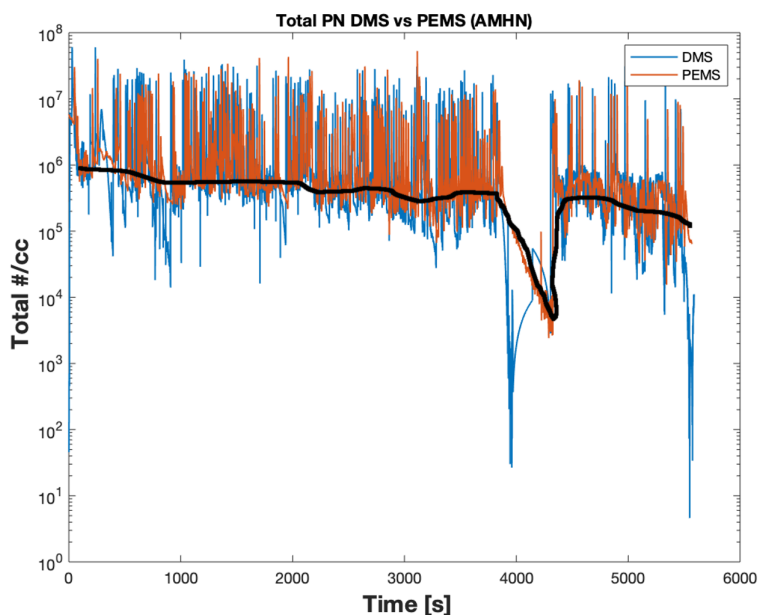


Figure 5.12: *PEMS vs DMS500 (AMHN) PN measurement comparison*

A common aspect in this figure is the "base" or the average PN value (highlighted by the dark line) for both instruments is of the same order of magnitude. The "peaks" or spikes in PN also seem to overlap. The peaks or the spike from average value in both figures correspond to engine starts mainly with few due to increase in power demand due to gradients and sudden accelerations. Since, the engine speed rises from 0 to approximately 2000 rpm (see figure 5.10) in a matter of seconds. It is at those few seconds when there is a rapid fuel enrichment leading to excess exhaust particles being measured at the tailpipe. It is known from studies that a GPF relies heavily on a buildup of ash layer which increases the degree of filtration [26]. This spike could be a result of insufficient ash layer formed as for such vehicles a minimum run mileage of 10000 km is required for enough build-up. Also filter regeneration can be another cause, when the soot cake formed on the walls lights off when the catalyst operates at high temperatures of 700 to 800°C whilst engine motoring or decelerating. Instances where despite fuel rate being fairly unchanged and noticing spikes in PN are observed.

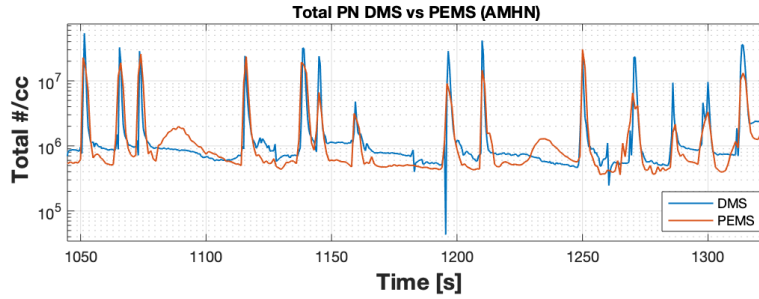


Figure 5.13: A zoom-in on figure 5.12

Figure 5.13 shows a zoom-in on the comparison and it is observed that the PEMS and DMS500 peaks overlap with minor inconsistencies. This helps strengthen the fact that both instruments are measuring similar amounts of particles with negligible errors. Although, some instances are found where a spike in DMS recording is seen and not in PEMS. A possible explanation to this would be owed to the volatility of the particles while travelling from the exhaust pipes through the probes and into the units. The temperature and pressure variations may cause some particles to disassociate into smaller sizes falling below the detection range of PEMS but well within that of DMS's. The following section will shed light on the particle size and propose possible explanations to such behaviours observed.

5.4.3 Particle Size Distribution

In this section, the size of the exhaust gas particles will be the main focus of analysis. By picking out few instances at different stages of the RDE tests the nature of the particles is studied to find any repeatable or varying traits in exhaust gas behaviour. This can only be achieved by using the DMS500 as it is capable of measuring the number of particles for each "size bin" as described in Section 3.3. Hence, this analysis is restricted to in-cell testing and the data from the same tests used for previous analysis is chosen to maintain uniformity in the results. The Figure 5.14 shows how the particle size along with PN varies during every peak. This is compared with the vehicle speed, engine speed, catalyst temperature, fuel rate and power (This is suspected to be when ICE propels the vehicle). The PN subplot data from the DMS500 is time-corrected to match with the PEMS dataset length to allow for a logical comparison. As seen from Figure 5.14 that the PN peaks usually occur at the points where engine speed rises rapidly and last only for few seconds.

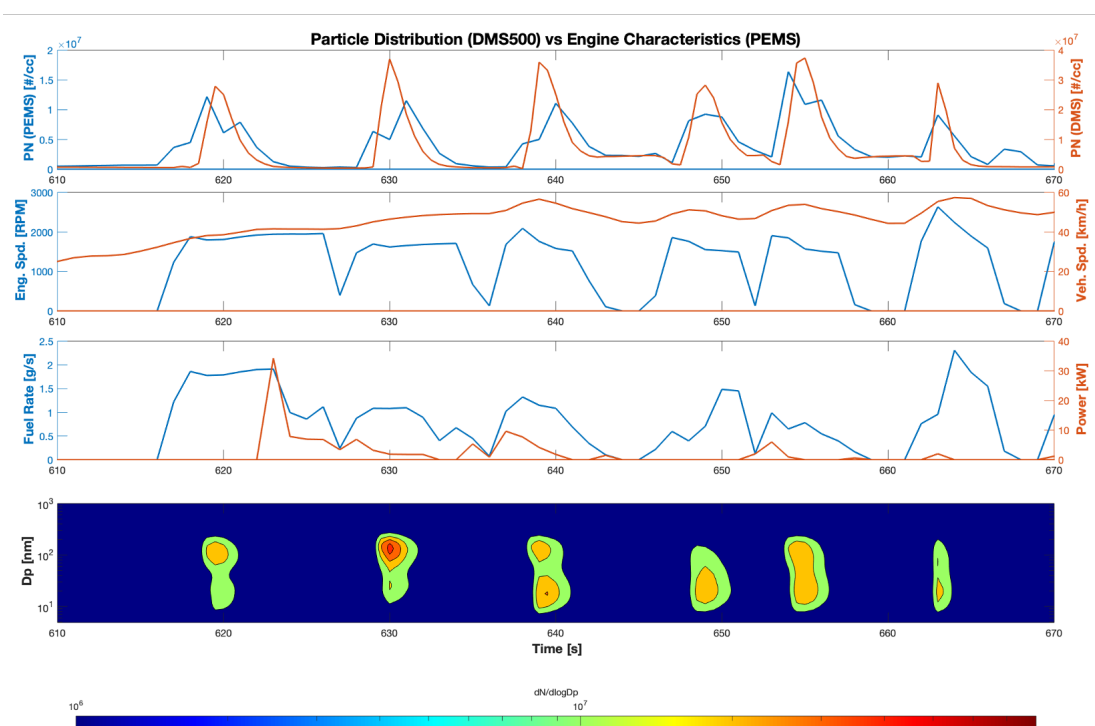


Figure 5.14: Particle size behaviour for frequent engine starts - AMHN

Here, the focus is on how the size of the particles varies despite the engine speeds corresponding to these peaks are fairly similar (see Figure 5.14) and the catalyst temperature (T_{cat}) suggests that it is operating near 'optimal efficiency'. It can be seen that majority of the particles lie above the 50nm size bin and this has been the majority case for numerous instances which are analysed by looking for any similar patterns. It can be concluded that majority of the particles emitted during the urban section of the trips lie in the 50 to 120 nm size range. Although this size does not qualify as 'large' but when compared to the rural and motorway sections this is true.

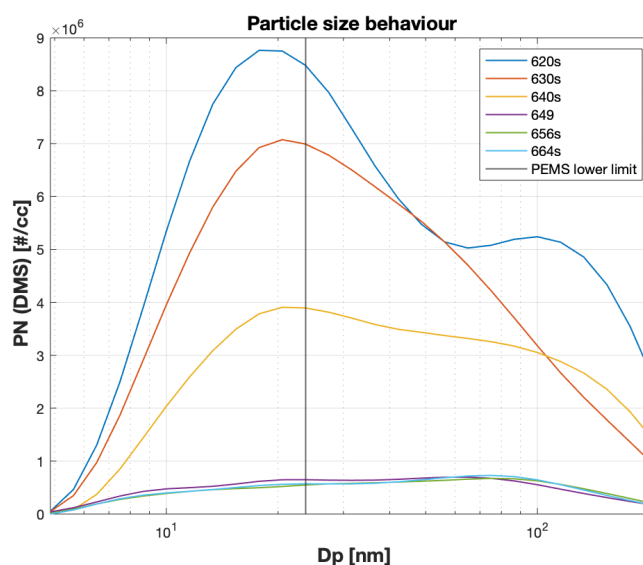


Figure 5.15: Size variation of peaks from fig 5.14

A PSD plot showing the size behaviour at each of these peaks shows how the nature of the particles changes in a matter of seconds (see figure 5.14). The first peak at 620 s shows particles of varied sizes from 5 to 200 nm seen by the blue line in Figure 5.15. This does not remain the case as we progress to the following peaks. The size distribution slowly shifts to beyond the 23 nm size leading to believe majority of the particles emitted at those instance were large and extend to sizes beyond 200 nm.

The remarks made from Figure 5.14 can also be seen in Figure 5.17. Here, this figure provides a good instance for multiple scenarios occurring in this short time frame. First, the spike in PN at the first engine start shows the DMS500 spike larger than the PEMS which can be owed to the particle size and detection range. Second, the spike at 3114 s shows the PEMS recording higher than the DMS500. This is in contradiction to the previous spike and its claim of the detection range explanation for measurement. Although, there lies another plausible explanation to this behaviour. It can be hypothesised that the particles being measured are not solid soot particles but in fact agglomerates of various compounds which upon entering the dilution stage of the DMS500 disintegrate. Where as in the PEMS, they are recorded due to the difference in the method of dilution and measurement between the two instruments. Thus, leading to such instances where the PEMS records higher PN than the DMS500. A PSD plot of three spikes at 3114 s, 3132 s and 3141 s for the same AMHN trip in Figure 5.16 shows how the size shifts drastically to the lower size range with around 50% of the particles being smaller than 23 nm in diameter. Despite the engine speeds, fuel rates and vehicle speeds remaining more or less the same there is stark difference in the size of particles, thus making it harder to conclude the what factor influences its behaviour. If it is due to the instruments or the particles and their volatility, a more in-depth analysis has to be done to know why their size varies of swiftly.

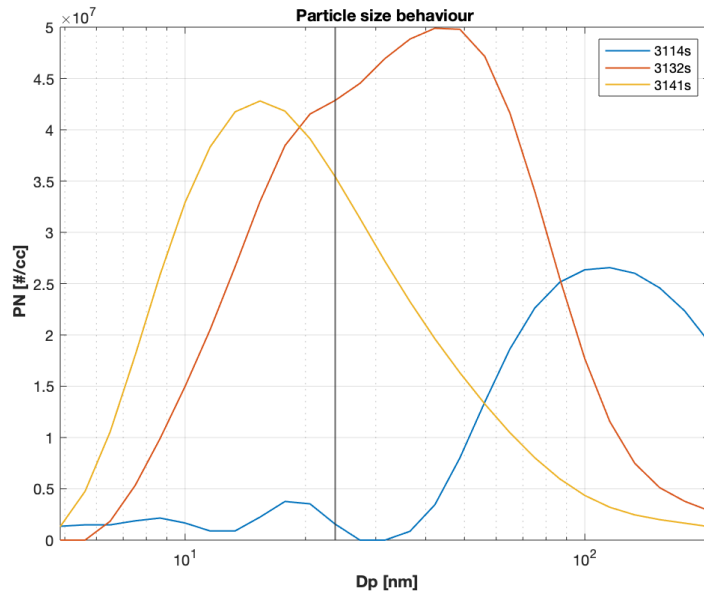


Figure 5.16: Size variation at 3114s, 3132s & 3141s in fig 5.17

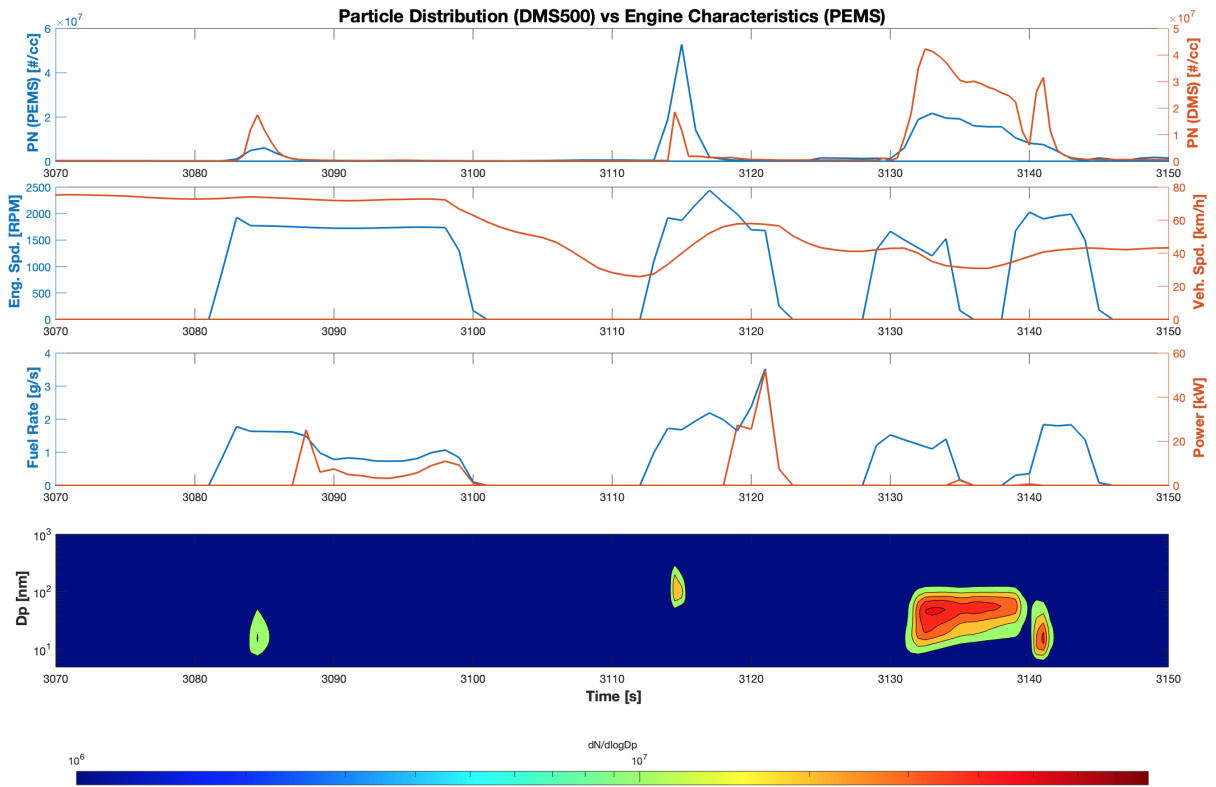


Figure 5.17: Particle size behaviour when PEMS and DMS record differently - Hilly

Raza M et al.[5] describes the morphology of unburned molecules from GDI engines and how they tend to agglomerate or adsorb other particulates downstream the engine which can then lead to PN multiplication or harmful compounds being formed in the atmosphere. Thus it is all the more important not to neglect these very fine particles.

The Figure A.17 summarizes the the average particle size for each section of the trips. The motorway section of the FLHC 1 trip is missing due to the issues occurred whilst performing this trip in the test cell. This illustration is made by closely observing the 3D contour plots for the sections of the tests performed in the test cell using the DMS. In Figures 5.18 & 5.19 it can be seen that majority of particles are smaller for rural and slightly larger for urban. Similarly, in Figure 5.20 majority of the particles are of smaller diameters with only few instances otherwise. The temperature of the catalyst is also varied at each of these sections of the trips and can be visualised in Figure 5.2. The catalyst on few occasions in motorway section is at a lower temperature compared to few instances in the urban sections. It cannot be said for certain if this attributed to the lower particle sizes observed in that section and since this was beyond the scope of this thesis it hasn't been investigated further.

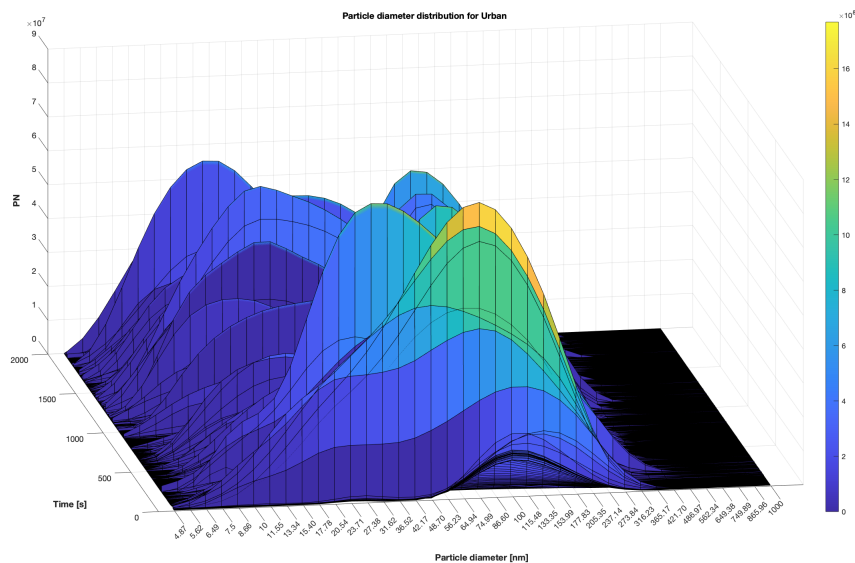


Figure 5.18: *PN Distribution in urban- test30*

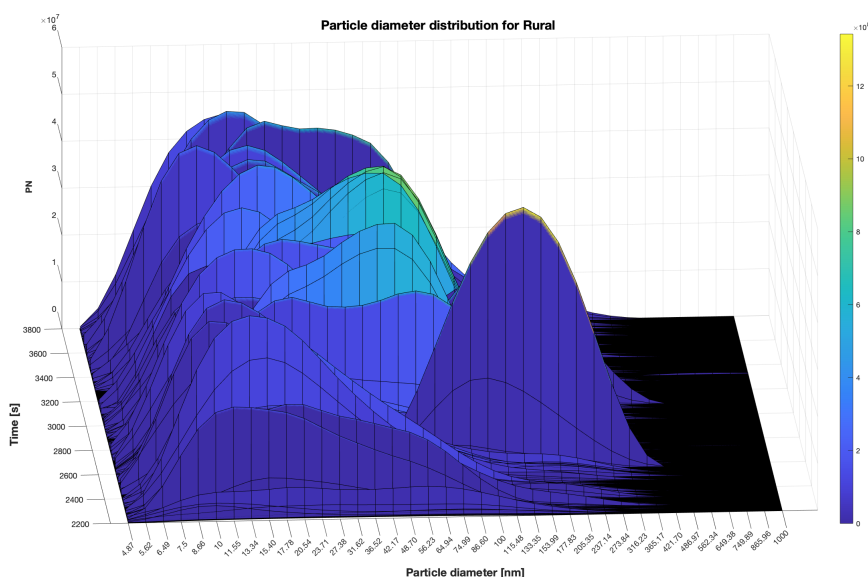


Figure 5.19: *PN Distribution in rural- test30*

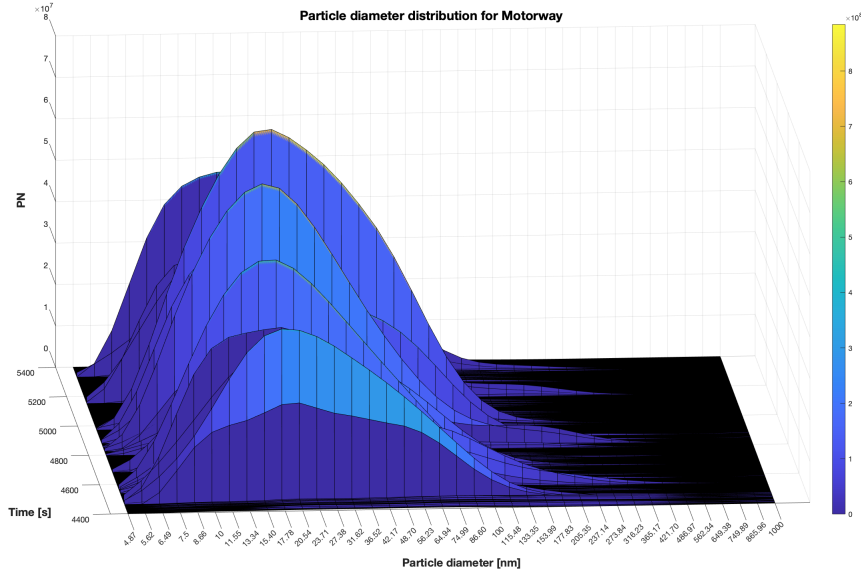
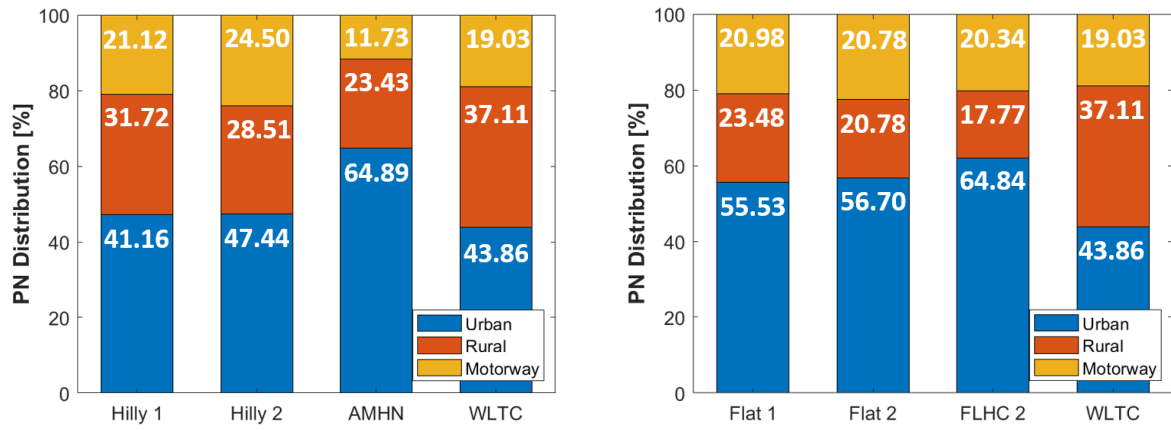


Figure 5.20: *PN Distribution in motorway- test30*

5.4.4 Comparison of On-road and In-cell RDE

This section of results is merely for studying the outcomes of two tests performed on different occasions and different vehicles. Despite the fact that the test performed in-cell (using 2018 data[24]) and on-road do not have the same purpose, they had a lot in common such as the vehicle type, test weather conditions, battery SoC level, engine start condition, driving routes and driving behaviour. Hence, this allowed us to compare the total PN for the flat and hilly driving routes.

Section 5 summarizes the emissions results from all tests. In order to have an objective comparison of PN distribution in each driving section, Figure 5.21 shows the percentage of PN distribution in each driving section. For hilly route, both on-road and in-cell testing has the same trend that particulate emitted mostly in urban section which is more than 45%. The second highest is in the rural following by the motorway. Comparing between on-road and in-cell testing, it can be observed that in-cell AMHN has emitted higher PN than the on-road testings in urban section and there is less PN distribution in the motorway section. Meanwhile, Hilly 1 and Hilly 2 have higher PN distribution on the rural and motorway sections than AMHN. For flat route, it follows the same trend of the hilly route as the highest PN distribution is in the urban. At the same time, the rural and motorway sections have similar value of the PN distribution which is approximately 21 to 25%. However, there is the contrast trend between the Hilly and Flat tests. In the Flat, the PN distribution in the rural is less than the motorway except for the Flat 1 (Only 3%). Comparing within only flat route testings, they all have similar value of the PN distribution unlike the hilly route testings that the PN distribution of the on-road and the in-cell testings are distinguishable.



(a) PN Distribution In Each Driving Section: Hilly Route (b) PN Distribution In Each Driving Section: Flat Route

Figure 5.21: PN Distribution In Each Driving Section of Hilly and Flat Route

Figure 5.22 shows a part of the urban section of Hilly route for both Hilly 2 and AMHN. A portion with speeds alike is chosen as there is closeness in vehicle and test conditions as mentioned earlier in the section. The nature of PN with respect to engine speed can be observed. The total PN is plotted and 'engine on' and 'engine off' parts of the plot can be distinguished with solid and dotted lines respectively. The average number of particles emitted at these urban stages is low between 1 to 5×10^7 (Figure 5.22) and this changes as the trip progresses.

In Figure 5.23, a part of the motorway section of FLHC 2 and Flat 1 is shown where there are more frequent engine starts that coincide with each step increase in speed. At these speeds the temperatures of the exhaust gases and catalyst are high and the EATS has a good filtration efficiency as most part of the trip has been completed. Furthermore, the total PN count speaks about the filtration efficiency of the GPF and the TWC.

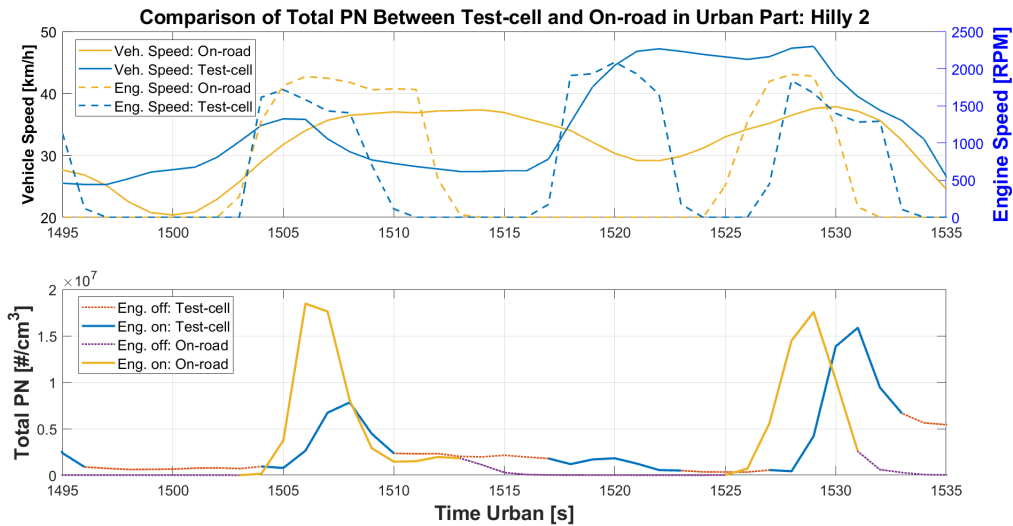


Figure 5.22: PN behaviour in urban section of Hilly route for same speeds between 2020 & 2018

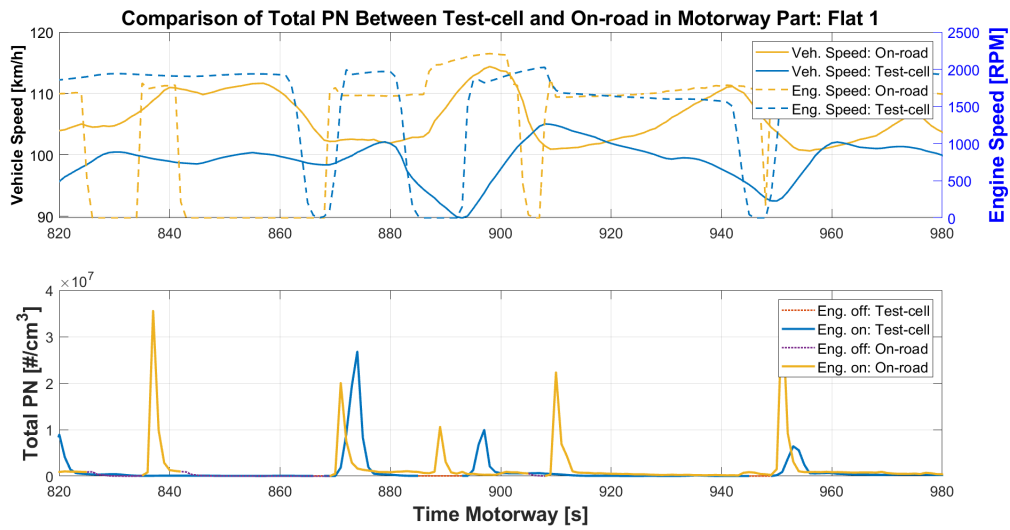


Figure 5.23: PN behaviour in motorway section of Flat route for same speeds between 2020 & 2018

For the flat RDE route, the total PN is also plotted with engine on and off mode. Overall, both of the tests have the same behavior as the hilly route where at every engine start point, the PN level will spike up. And when engine is off, the PN level decreases or drops to zero level. At the similar vehicle speed, the total PN level of the on-road RDE (Flat 1) trip is higher than test-cell (FLHC 2) in rural and motorway section as shown in Figure 5.24 and A.13. However, the trend of urban section is slightly different than in another two parts. As at some significant times, the total PN level of test-cell (FLHC 2) are higher than on-road RDE trip. The behaviour of the PN can be also related to engine speed. Even though both of the tests have similar speed profile but the engine speed is undoubtedly different as in Figure 5.23. Since, these tests were performed using different vehicles, their individual engine requests can never be similar, thus resulting in the different PN behaviour.

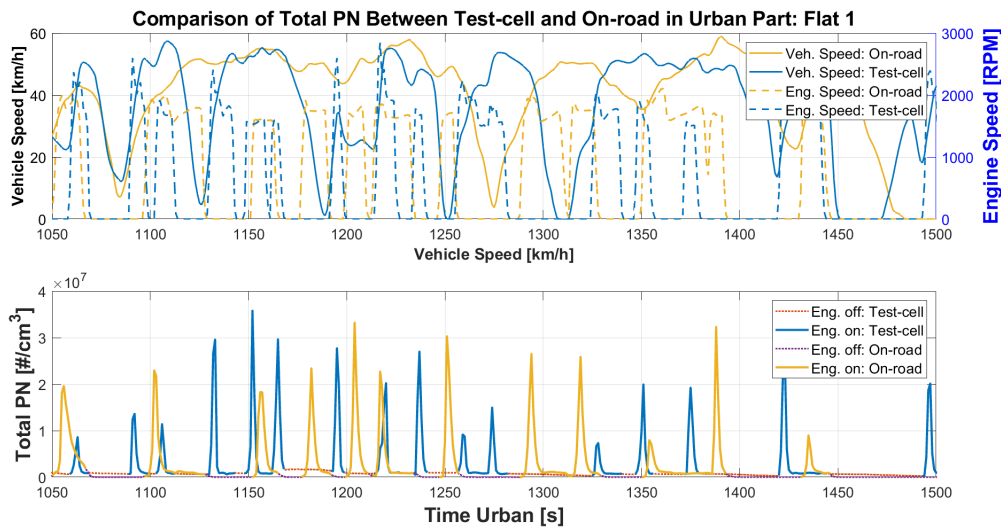


Figure 5.24: PN behaviour in urban section of flat route for same speeds between 2020 & 2018

5.5 Effects of Driving Aggressiveness

Driving Aggressiveness has played an important role on emissions and fuel consumption of the vehicle. It is measured and calculated in terms of 'vapos₉₅' which is 95th percentile of $v \cdot a$ (speed \times positive acceleration).

It indicates the degree of driving behaviour and it is also the metric of high dynamic boundary condition. According to RDE requirement, the trip dynamic shall not be too smooth, the low dynamic boundary condition is also taken into account. RPA or Relative positive acceleration is introduced as a low dynamic boundary condition and RPA per speed bin can be calculated Equation 5.1 [COMMISSION6].

$$RPA_k [m/s^2] = \frac{\sum_j (\Delta t [s] \times (speed [m/s] \times positive\ acceleration [m/s^2])_{j,k}}{\sum_i d_{i,k} [m]} \quad (5.1)$$

where $j = 1$ to M_k , $i = 1$ to N_k , $k =$ urban, rural, motorway, $RPA_k =$ RPA for urban, rural, and motorway shares, $\Delta t =$ time difference equal to 1 second, $M_k =$ the sample number for urban, rural and motorway shares with positive acceleration, and $N_k =$ the total sample number for urban, rural and motorway shares.

In Table 5.4, the aggressiveness of every driving section of in-cell RDE tests on each trip are compared with on-road RDE trips for this study. For the in-cell AMHN and FLHC 2, the aggressiveness value is high, close to the upper limit for every driving section. Whereas for the 2020 trips it is less half of the in-cell tests. However, for total aggressiveness, the $vapos_{95}$ values of the 2020 trips are not much lower than the in-cell as they are in the driving sections. However, even if the vehicle was driven by Sahil is less aggressive than the 2018, the PN emission is still higher. It can suggest that the driving aggressiveness does not have an influence on exhaust emissions but more important factor is engine's operation.

Table 5.4: Dynamic Boundary Conditions of On-road RDE and Test-cell RDE On Each Driving Section

Trip	Dynamic Boundary Condition	Urban	Rural	Motorway	Total
	Vapos95 limit [m^2/s^3]	<18.7	<24.3	<26.6	-
	RPA limit [m/s^2]	>0.13	>0.06	>0.03	-
AMHN	vapos ₉₅	12.50	15.10	9.90	23.06
	RPA	0.21	0.08	0.04	-
Hilly 1	vapos ₉₅	9.60	12.90	10.90	12.45
	RPA	0.18	0.08	0.05	-
Hilly 2	vapos ₉₅	8.90	12.90	14.00	12.60
	RPA	0.18	0.06	0.07	-
FLHC 2	vapos ₉₅	13.00	16.80	16.30	18.20
	RPA	0.18	0.08	0.04	-
Flat 1	vapos ₉₅	9.80	14.10	12.50	14.97
	RPA	0.22	0.09	0.10	-
Flat 2	vapos ₉₅	10.50	12.90	10.00	12.39
	RPA	0.19	0.08	0.05	-

Figures 5.25a & 5.25b illustrate the nature of distribution of the vapos samples between tests performed both in-cell and on-road. Since, the in-cell tests were the same as the 2018 thesis which had a high aggressiveness, this can be seen in these figures. Even if both of the histograms are right-skewed, the Flat 2 has its peak concentration towards the lower value of vapos more than the the FLHC 2 in Figure 5.25a. The same can be said regarding Figure 5.25b despite it appearing to have the peaks coinciding. In the high vapos region, the number of samplings of the in-cell are significantly higher than the on-road. This means the accelerations of the on-road is less than the in-cell, hence, the less aggressiveness of the on-road RDE tests. There are many samples which have a high vapos value but due to low number of samples at those values they are virtually hidden in this plot. The 95th percentile value provides evidence for this. Nevertheless, during the test, the System Control's RDE-online indicated the green light for vapos₉₅ and RPA to validate the driving test.

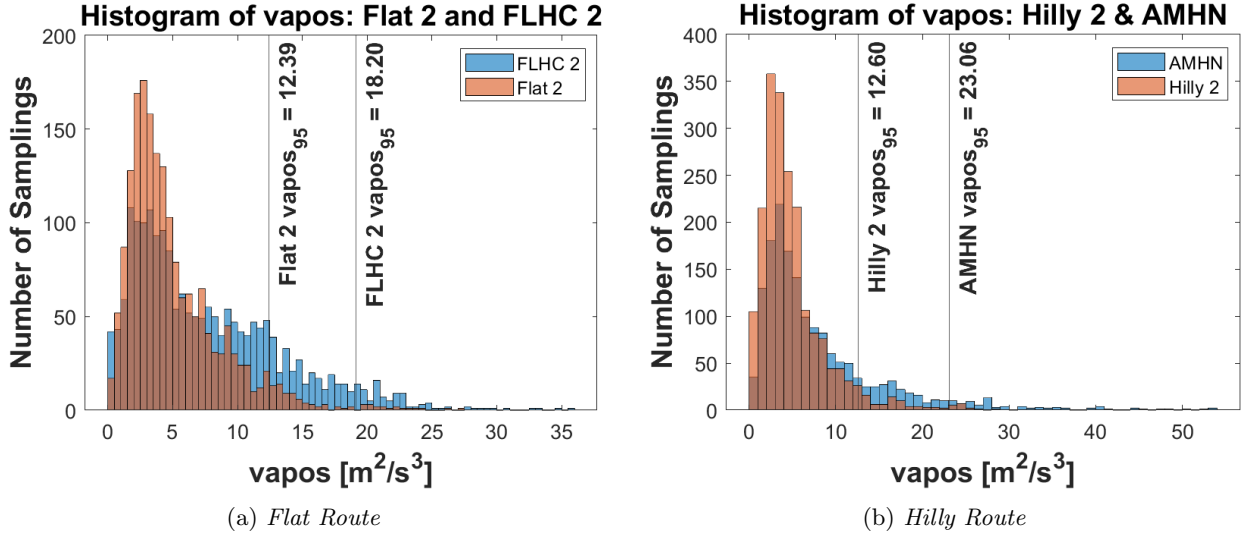


Figure 5.25: Histogram of Aggressiveness ($vapos_{95}$) of In-cell and On-road

5.6 Residence Time

The residence time (τ [s]) is described as the amount of time spent by a particle to travel through the specified control volume of interest. Normally, there is a time-lag in data measurement between the ECU and PEMS, since there is a distance from the engine to the PEMS. Thus, the data in PEMS was logged few seconds later compared to the ECU. This delay is given by the distance that the gases must travel before being measured i.e. residence time which in-turn depends on the fuel rate and temperature of the exhaust gas. At lower engine speeds, the gas temperature is less, thus, resulting in higher times than at faster speeds. The same logic applies to the rate of fuel injected into the engine.

The residence time can be calculated by the ratio of volume of the exhaust system from engine out to PEMS probe to the volume calculated by universal gas law using data from PEMS. \dot{V} [m^3/s] in equation 5.2 is the volume calculated from gas law, \dot{m} is fuel rate [g/s], R is universal gas constant 8.31441 [J/mol/K], T_{exh} is exhaust gas temperature [K] and p_{atm} is ambient pressure [Pa]. V_{sys} [m^3] in Equation 5.3 represents volume of exhaust system [m^3] where r is average radius of exhaust pipe [m] and L is the approximate length of exhaust system measured from engine out to the PEMS probe combined with $V_{catalyst}$ and $V_{muffler}$ is volume of catalyst and muffler respectively [m^3].

$$\dot{V} = \frac{\dot{m}RT_{exh}}{P_{atm}} \quad (5.2)$$

$$V_{sys} = \pi r^2 L + V_{catalyst} + V_{muffler} = 0.015 + 0.013 + 0.0029 = 0.0309 \quad (5.3)$$

$$\tau = \frac{V_{sys}}{\dot{V}} \quad (5.4)$$

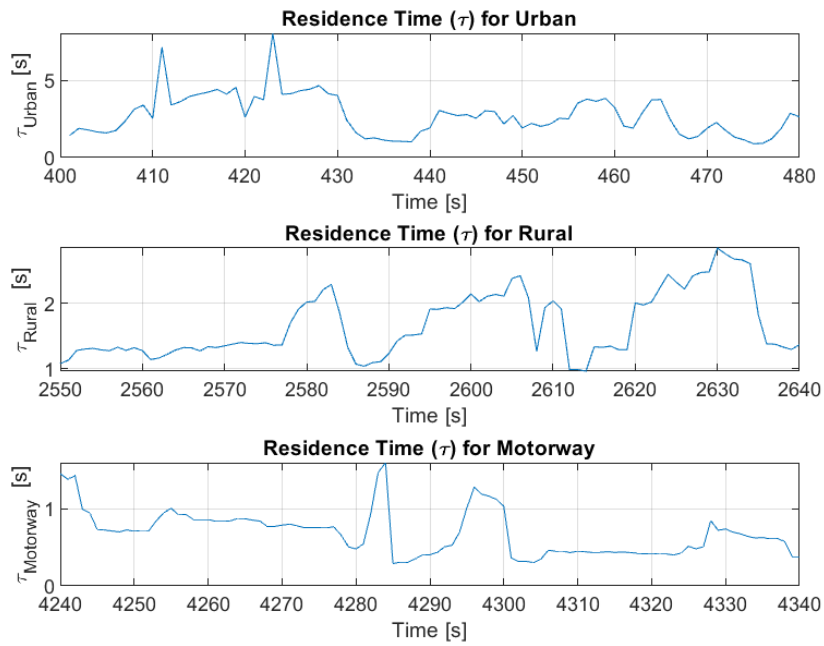


Figure 5.26: *Residence time on each driving sections*

Figure 5.26 shows the example of the residence time in urban, rural, and motorway part from the trip Hilly 1. The residence time of urban is 3 to 5 seconds, the rural part is 1 to 2 seconds and the motorway is 0.5 to 1.5 seconds. The first observation is the residence time reduces as vehicle speed increases.

6 Conclusion

The RDE tests as well as a standard driving cycle; WLTC using a gasoline PHEV were conducted to study about the behaviour of NO_x and particulate emissions. The tests were performed in a test-cell and on-road in Gothenburg for 2 different road profiles; flat and hilly.

The exhaust emissions are affected by the operations of the engine. In this thesis study found that the NO_x is relatively low but its behaviour can be still analysed. Generally, NO_x is released at the beginning of the trip or at the engine-start point. These are because at the beginning of the trip or before the engine starts, the catalyst is cold and requires an adequate temperature to be effective in reducing the NO_x CO and HC. However, when the catalyst reached its effective point, there were still high levels of CO being recorded which proves that the TWC was in fact not operating at the ideal state. The lambda sensor is believed to have been non-operational causing the engine to run rich all the time which can also justify the low NO_x levels.

Particulate emissions heavily depends on the number of engine starts as there are more spikes in PN observed coinciding with every engine start. The time of engine operation has also been a factor for the PN level. Even if the peak of the particle occurs at every engine start, the small level of the PN tail still exists when the engine is continuously running. These amount of particles can accumulate and contribute to the high level of the PN. The behaviour of the PN can also be explained by fuel demand of the engine. When the engine starts, high amount of fuel is injected. With this fuel enrichment, the level of the PN surges up as the result of the transient state of engine.

The particulate results from PEMS and DMS500 match on most occasions with minor inconsistencies. With different measurement instruments and techniques for both instruments, the inconsistencies are bound to occur. The fine particles below the 23 nm range are thought to be volatile particles which sometimes disintegrate inside the DMS500 due to its two-step dilution process however get recorded in the PEMS as its technique varies. Thus, resulting in instances where PEMS measures more than the DMS500. The DMS500 has a wider detection range than PEMS, so, the smaller sizes (less than 23 nm) of particle are captured by DMS500 and they are occasionally released during the test. These small particles should be taken into account, since they are highly volatile and agglomerate to form bigger particles which in turn leads to increase in PN level.

The driving aggressiveness study has shown an unexpected result because with lower aggressiveness of the on-road RDE tests, the PN level of the on-road tests are still higher than the in-cell tests which has twice the aggressiveness. This can be concluded by the fact that the particulate emission most likely relates to engine operation than the aggressiveness. In order to have a strong conclusion about aggressiveness, it is interesting to perform more tests with more aggressive driving behaviour for the on-road RDE test.

The peculiar behaviour of the PEMS has played an important role, since there were some "bumps" recorded in the PN logging which occurred during engine-off periods. Such activity is rather unusual and an in-depth study of PEMS measurement procedure can be useful for future research work to have accurate understanding of the results. Moreover, for the future emissions regulations the conformity factor of the RDE test will possibly be reduced to a value that is close to 1, which means there is no allowance in the uncertainty of measurement for RDE test.

For further studies, it will be interesting to perform more RDE tests and also tests with different EATS combinations. The process of achieving repeatability in testing is very crucial to make valid conclusions about the emissions since these tests are performed in real life scenarios where consistency is scarce. The use of different fuels along with other hybrid modes will also be insightful. The test vehicle used for this study was different from a typical production vehicle. Hence using a vehicle that is also used by the masses for testing may prove to be conclusive in terms of emission nature and behaviour. If future research paves the way for actual emissions behaviour to be studied closely and develop powertrain control strategies, only then will there be a positive impact of the legislation and the effort towards a cleaner future.

References

- [1] European Commission and Council of the European Union. Commission Regulation (EU) 2016/427 of 10 March 2016 amending Regulation (EC) No 692/2008 as regards emissions from light passenger and commercial vehicles (Euro 6) (Text with EEA relevance). *Official journal of the European Union* (2016).
- [2] Rui Chen et al. Beyond PM_{2.5}: The role of ultrafine particles on adverse health effects of air pollution. *Biochimica et Biophysica Acta (BBA) - General Subjects* **1860.12** (2016), 2844–2855. ISSN: 0304-4165. DOI: <https://doi.org/10.1016/j.bbagen.2016.03.019>. URL: <http://www.sciencedirect.com/science/article/pii/S0304416516300745>.
- [3] J.B. Heywood. *Internal Combustion Engine Fundamentals, Second Edition*. 2018. ISBN: 9781260116106.
- [4] *Polycyclic aromatic hydrocarbons (PAHs)*. URL: <https://www.kemi.se/en/prio-start/chemicals-in-practical-use/substance-groups/polycyclic-aromatic-hydrocarbons-pahs>.
- [5] Mohsin Raza et al. A Review of particulate number (PN) emissions from gasoline direct injection (gdi) engines and their control techniques. *Energies* **11.6** (June 2018). ISSN: 19961073. DOI: 10.3390/en11061417.
- [6] V Castranova et al. Effect of exposure to diesel exhaust particles on the susceptibility of the lung to infection. *Environmental Health Perspectives* **109**.suppl 4 (Aug. 2001), 609–612. DOI: 10.1289/ehp.01109s4609. URL: <https://doi.org/10.1289/ehp.01109s4609>.
- [7] David B Kittelson. Engines and nanoparticles: a review. *Journal of Aerosol Science* **29.5** (1998), 575–588. ISSN: 0021-8502. DOI: [https://doi.org/10.1016/S0021-8502\(97\)10037-4](https://doi.org/10.1016/S0021-8502(97)10037-4). URL: <http://www.sciencedirect.com/science/article/pii/S0021850297100374>.
- [8] Martin Lenz et al. A case study on particulate emissions from a gasoline plug-in hybrid electric vehicle during engine warm-up, taking into account start–stop operation. *Proceedings of the Institution of Mechanical Engineers, Part D: Journal of Automobile Engineering* (2020). ISSN: 09544070. DOI: 10.1177/0954407020931227.
- [9] Katherine E. Zychowski et al. Vehicular Particulate Matter (PM) Characteristics Impact Vascular Outcomes Following Inhalation. *Cardiovascular Toxicology* **20.3** (June 2020), 211–221. ISSN: 15590259. DOI: 10.1007/s12012-019-09546-5.
- [10] Olga V. Lozhkina and Vladimir N. Lozhkin. Estimation of nitrogen oxides emissions from petrol and diesel passenger cars by means of on-board monitoring: Effect of vehicle speed, vehicle technology, engine type on emission rates. *Transportation Research Part D: Transport and Environment* **47** (Aug. 2016), 251–264. ISSN: 13619209. DOI: 10.1016/j.trd.2016.06.008.
- [11] Aecc. *Gasoline Particulate Filter(GPF) How can the GPF cut emissions of ultrafine particles from gasoline engines?* Tech. rep. 2017.
- [12] Xunmin Ou and Xiliang Zhang. Life-Cycle Analyses of Energy Consumption and GHG Emissions of Natural Gas-Based Alternative Vehicle Fuels in China. *Journal of Energy* **2013** (2013). Ed. by Qilian Liang, 268263. ISSN: 2356-735X. DOI: 10.1155/2013/268263. URL: <https://doi.org/10.1155/2013/268263>.
- [13] Yisong Chen et al. *Emissions of automobiles fueled with alternative fuels based on engine technology: A review*. Aug. 2018. DOI: 10.1016/j.jtte.2018.05.001.
- [14] Mustafa Kemal Balki, Cenk Sayin, and Mustafa Canakci. The effect of different alcohol fuels on the performance, emission and combustion characteristics of a gasoline engine. *Fuel* **115** (2014), 901–906. ISSN: 00162361. DOI: 10.1016/j.fuel.2012.09.020.
- [15] *dieselnet_EU_emission standards*. URL: <https://dieselnet.com/standards/eu/index.php>.
- [16] Peter Mock. *Real-driving emissions test procedure for exhaust gas pollutant emissions of cars and light commercial vehicles in Europe*. Tech. rep. 2017.
- [17] *The development of RDE in Europe RDE IWG kick off meeting*. Tech. rep. 2018.
- [18] *I implementing and amending Regulation (EC) No 715/2007 of the European Parliament and of the Council on type-approval of motor vehicles with respect to emissions from light passenger and commercial vehicles (Euro 5 and Euro 6) and on access to vehicle repair and maintenance information (Text with EEA relevance)*. Tech. rep. 2008.
- [19] *AVL Gas PEMS iS Product Guide*. Tech. rep.
- [20] *AVL PN PEMS iS Product Guide*. Tech. rep.
- [21] *Procedure for measuring real driving emissions of contestants*. Tech. rep. 2017.
- [22] *Users Guide*. Tech. rep. 2016.
- [23] *DMS particle analyser*. URL: <https://www.cambustion.com/products/dms500/engine>.

- [24] Luvid Andersson and Mohammed Saeed. *Real Driving Emissions (RDE) of a Gasoline PHEV*. 2018. URL: <https://hdl.handle.net/20.500.12380/256029>.
- [25] Musaab O. El-Faroug et al. *Spark ignition engine combustion, performance and emission products from hydrous ethanol and its blends with gasoline*. Dec. 2016. DOI: 10.3390/en9120984.
- [26] Tak W. Chan et al. Characterization of Real-Time Particle Emissions from a Gasoline Direct Injection Vehicle Equipped with a Catalyzed Gasoline Particulate Filter During Filter Regeneration. *Emission Control Science and Technology* **2.2** (Apr. 2016), 75–88. ISSN: 21993637. DOI: 10.1007/s40825-016-0033-3.

A Appendix

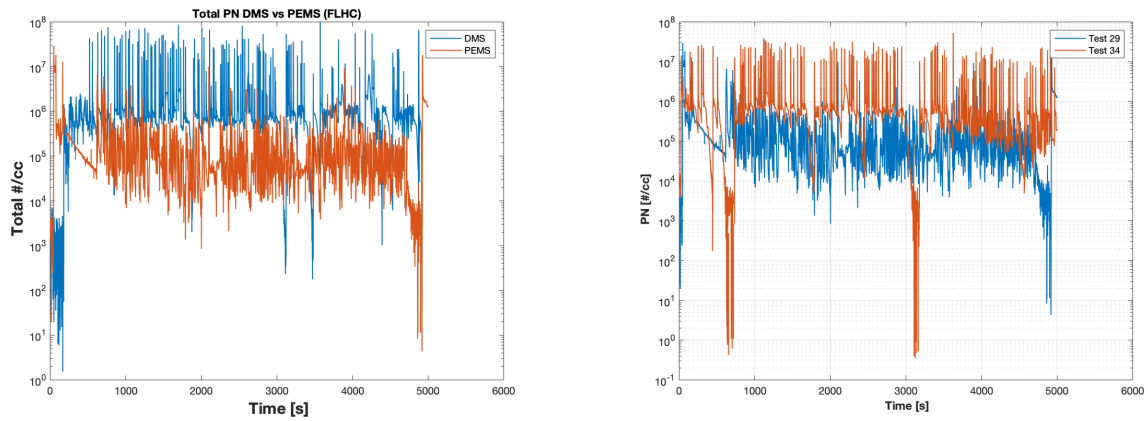
A.1 Discussion On Measurement Error In Test-cell

In Table A.1 is the results summary for FLHC 1. As it is mentioned in the result and discussion section that FLHC 1 is the test which was incomplete thus making it unsuitable for discussion. So, the emissions result can be only presented for urban and rural section.

Table A.1: Emissions Summary for Test-cell RDE: FLHC 1 (Test 29)

Emission	Unit	FLHC 1
Test Order	-	Test 29
NO_x	-	-0.09
NO_x Motorway	-	-
NO_x Rural	-	-6.35
NO_x Urban	-	-0.01
PN	-	0.32
PN Motorway	-	-
PN Rural	-	0.14
PN Urban	-	0.33
Trip Duration	s	5003
Trip Distance	km	50.96

The trend of the total PN between DMS500 and PEMS of the FLHC 1 is remarkably different. As in Figure A.1a, DMS500 has recorded higher PN than PEMS as contrast with the expectation that the PN level from both measurement should have the same or similar level and trend. Moreover, Figure A.1b does not show similar trends between the test 29 and the test 34 which was driven the same driving cycle as the test 29. Despite the fact that the test 29 is shorter than the test 34 by an approximate 15 minutes due to the fact that there were many disruptions while carrying out this test in the test-cell, for the same period of time, the PN level of the test 29 should have been the same level as the test 34. However, it is the best available data set from all the tests for the flat route (FLHC 1) which also has DMS500 data.



(a) PN comparison between DMS500 and PEMS of FLHC 1 (Test 29) (b) PN comparison between FLHC 1 (Test 29) and FLHC 2 (Test 34)

Figure A.1: Comparison of PN

Test 34 is one amongst the many tests carried out in the test-cell with the flat route (FLHC). This test completed the full cycle without any interruptions but without the DMS500. Hence, this test was not selected for the result analysis part for DMS500 and PEMS comparison. When test 34 is compared with test 29, the true PN behaviour is noticed in test 34 which ran completely with the vehicle exhibiting true 'hybrid' behaviour with more engine starts as compared with test 29 as in Figure A.2.

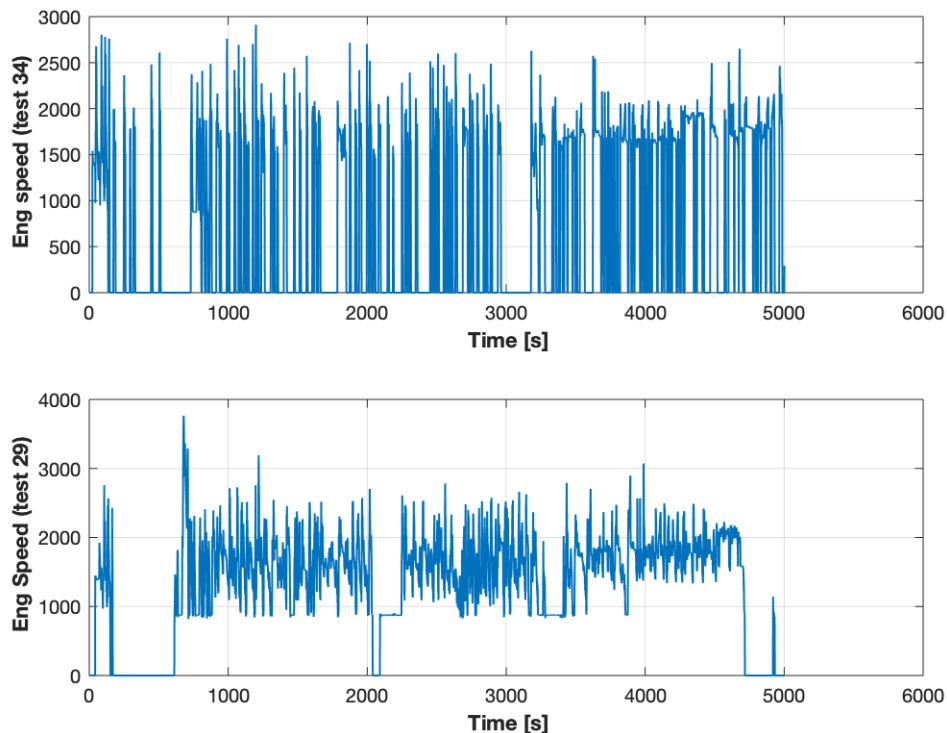
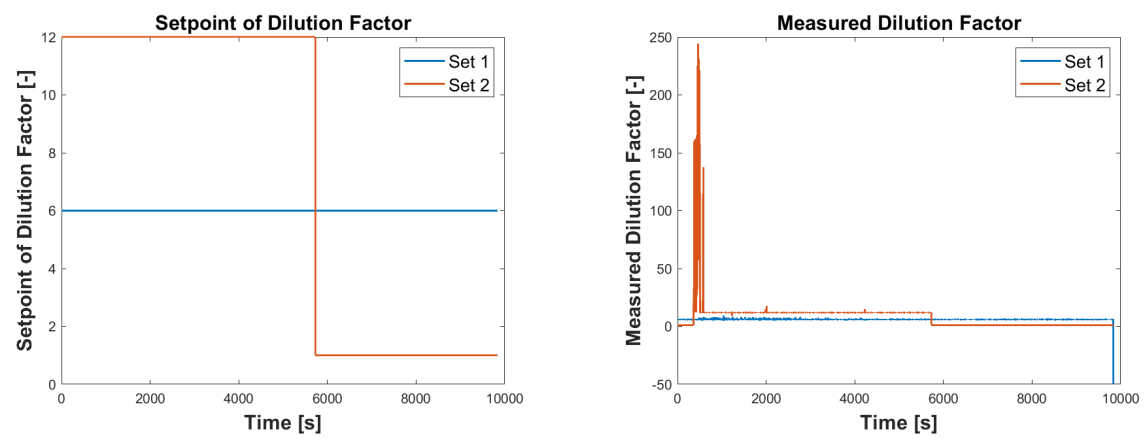


Figure A.2: Engine speed comparison between Test 29 & 34

Figure A.3 shows the measured and set-point value of the dilution factor in DMS500. It can be seen that the dilution factor was set as 6 for the dilution set 1 and 12 for the dilution set 2. However, there was a change in the dilution set-point for set 2 to be 1 during the test. As for the measured dilution factor, there

was a big spike of the measured dilution during 360 s to 500 s. Apart from this timestamp, it seems that the dilution had been worked properly. The change in set-point of dilution factor and the spike of the measured dilution factor can be reasons which cause the high difference on PN level of the DMS500 and PEMS.



(a) Setpoint of Dilution Factor (b) Measured Dilution Factor
 Figure A.3: Comparison of Dilution Factor between Setpoint and Measured Value

A.2 Abnormal behaviour in PEMS PN measurement

During the close analysis of the results it was observed that the PN recorded from the PEMS had frequent "bumps" in the PN when plotted on a logarithmic scale. Upon an in-depth analysis it was observed that these occur mainly during engine-off periods when no fuel is injected into the engine. Figures A.5a and A.5b show a few such instances where this is noticed.

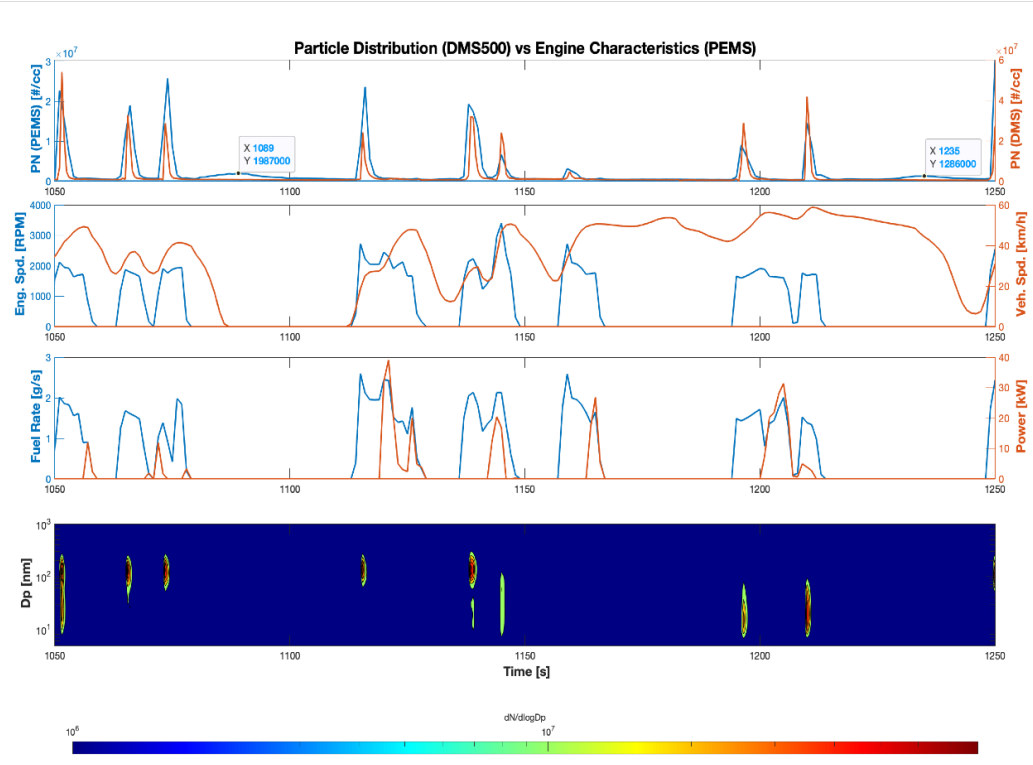


Figure A.4: PEMS PN abnormality: Instance 1

Their corresponding contour plots in Figures A.4 and 5.17 show the state of the engine speed and fuel rate at these instances in time. This strengthens the claim that this behaviour is PEMS oriented and not contributed in any way by the vehicle exhaust gas. The reasoning behind this behaviour is not certain but can be owed to the operating characteristics or settings on the PEMS. A closer study of the unit has to be done to understand why this occurs frequently just before or after a spike is recorded.

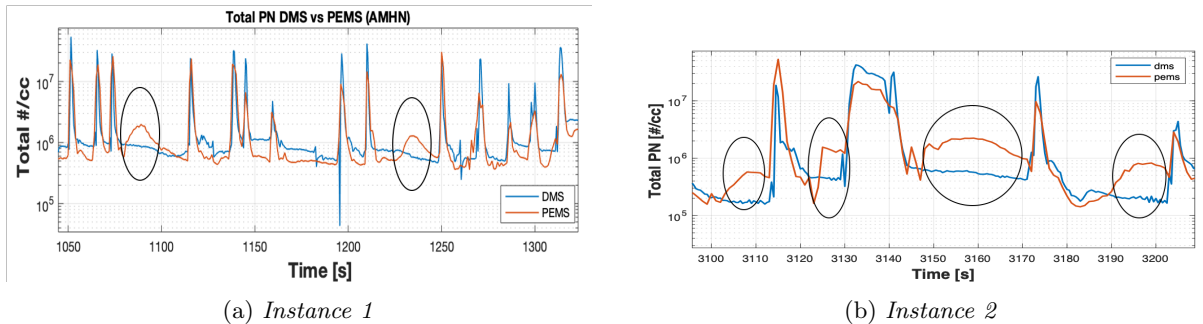


Figure A.5: Comparison of Dilution Factor between Setpoint and Measured Value

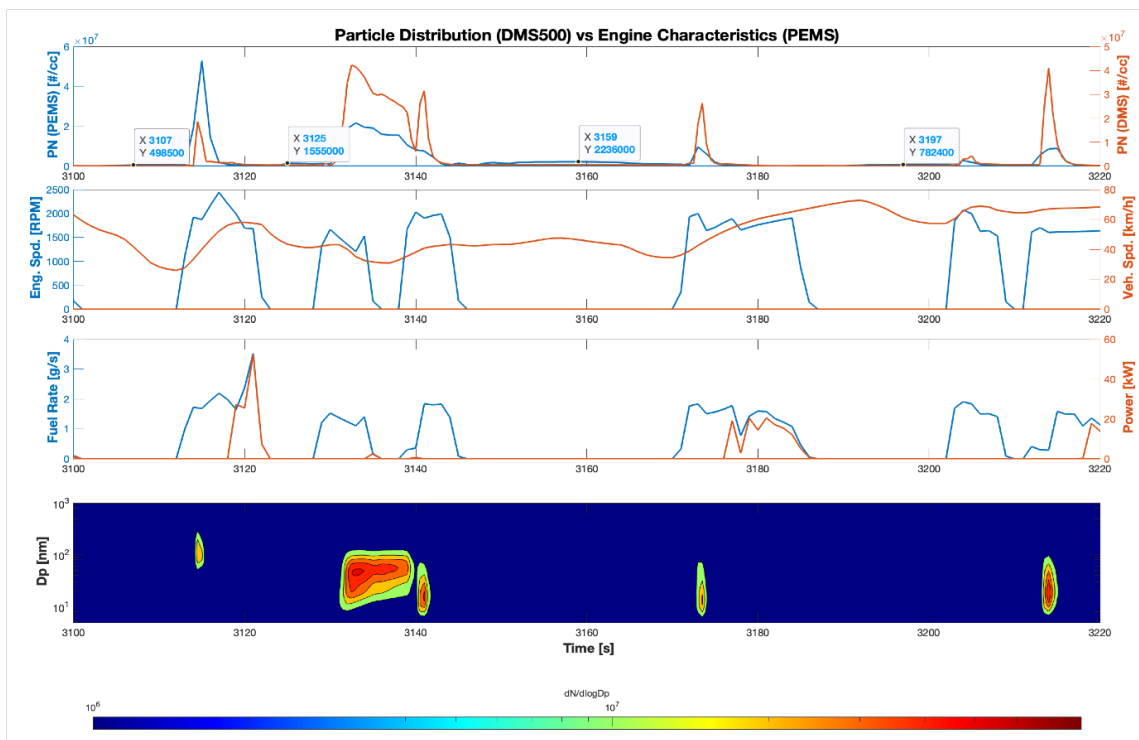


Figure A.6: PEMS PN abnormality: Instance 2

Table A.2: Integrals of few bumps recorded in PEMS

Time frame [s]	Total PN Integral [#/cc]
1081-1100	2.646E+7
1229 -1246	1.639E+7
3102 - 3113	4.552E+6
3147 - 3172	4.183E+7
3188 - 3203	8.627E+6

In table A.2 below the instances mentioned earlier are taken and the period of each bump is integrated

to know how much erroneous PN is contributed by these bumps to the total PN. Most of these bumps last for an average of 8 to 10 seconds with few lasting as long as 25 seconds. From Table A.2 it can be said that these bumps have a minor contribution to the total PN, although if found to occur many times could prove to be damaging to the result analysis. It is difficult to manually identify all of these instances and check for their contribution to the total PN.

A.3 Residence time

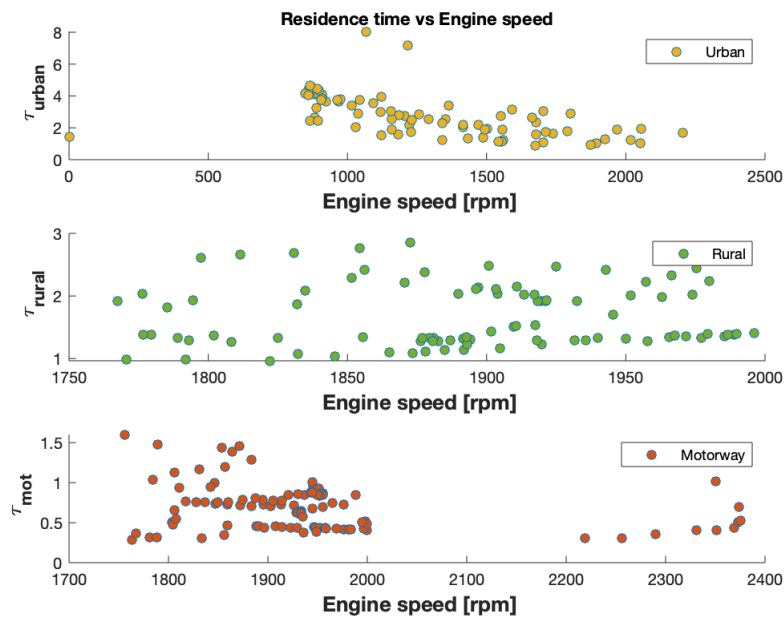


Figure A.7: Residence Time vs Engine Speed (AMHN)

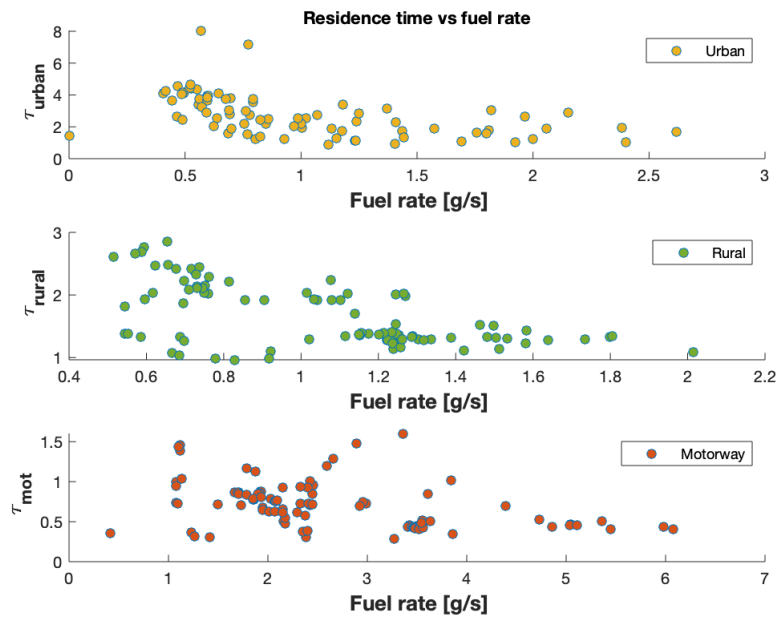


Figure A.8: *Residence Time vs Fuel Rate (AMHN)*

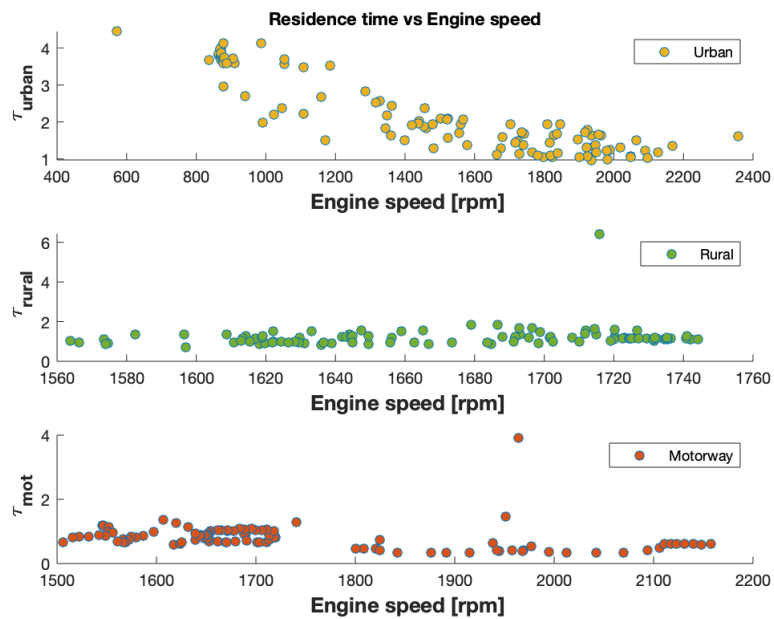


Figure A.9: *Residence Time vs Engine Speed (FLHC)*

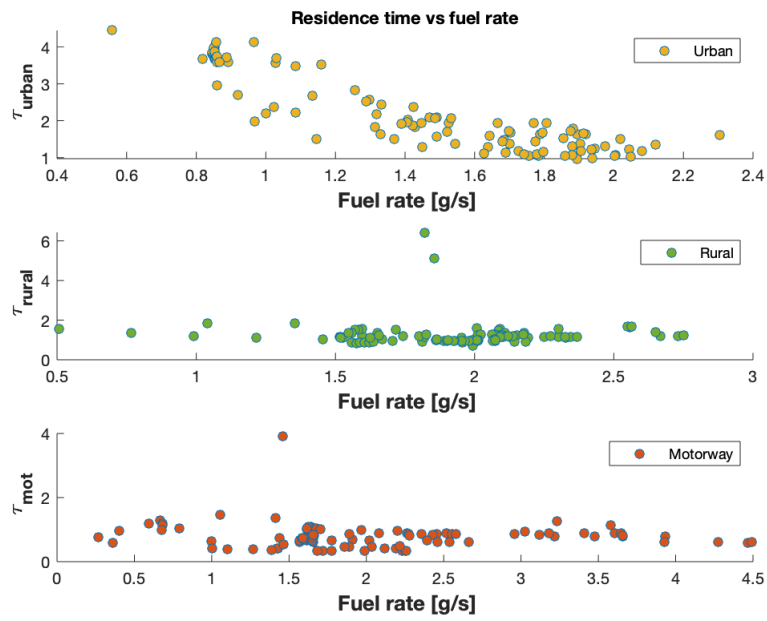


Figure A.10: Residence Time vs Fuel Rate (FLHC)

A.4 Standard Cycle WLTC

A.4.1 NO_x

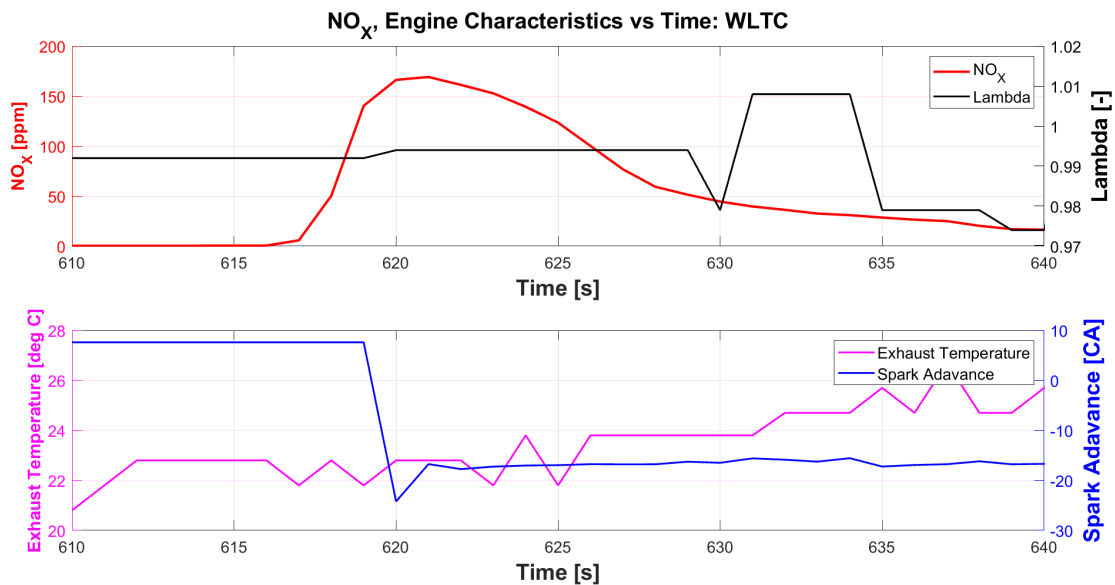


Figure A.11: Peak of the No_x with 1500 RPM Engine Speed

A.5 Emissions of Flat 1 Route

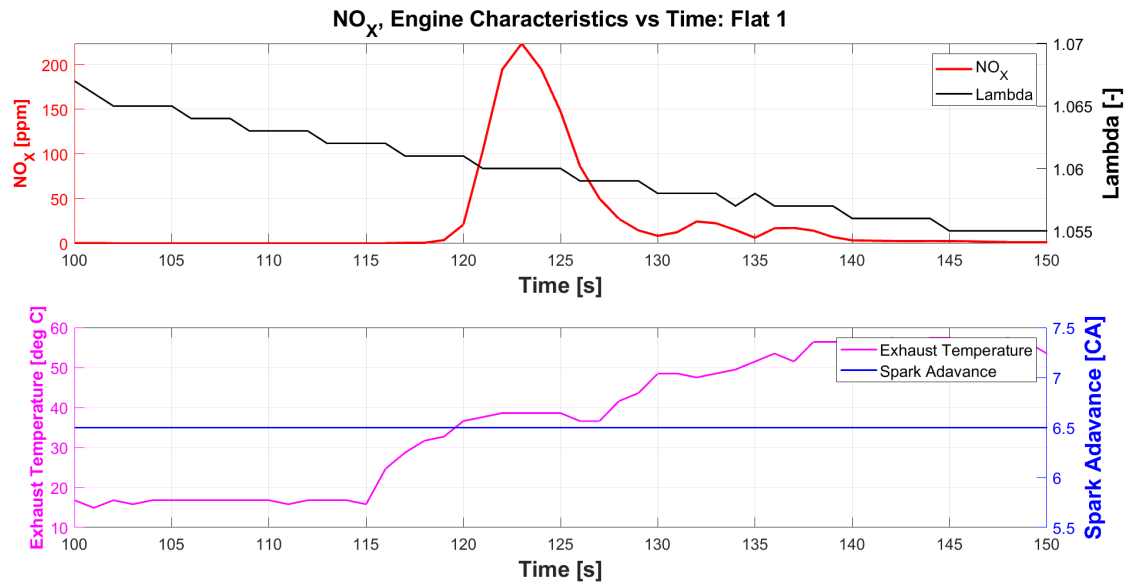


Figure A.12: Peak of the No_x with 2000 RPM Engine Speed

A.5.1 Particle Number

Comparison of Total PN between Test-cell and On-road

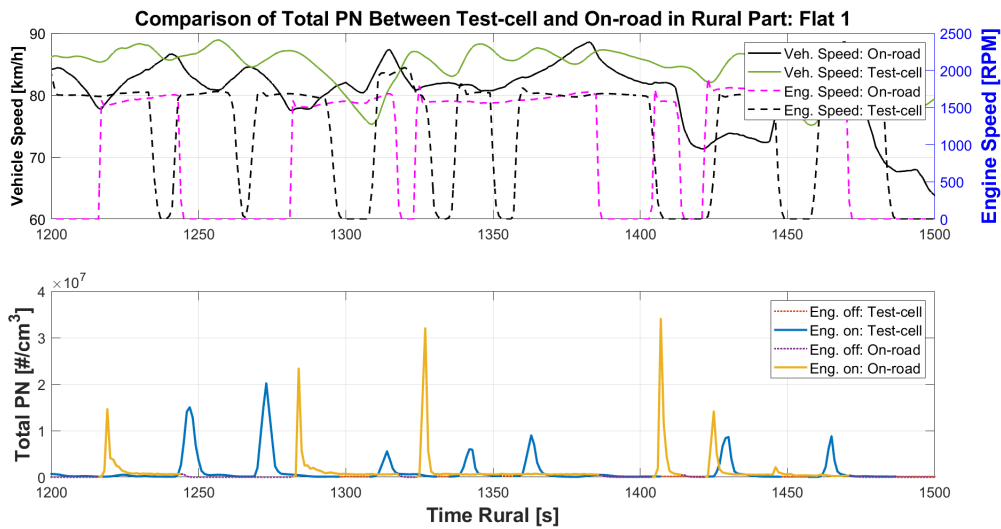
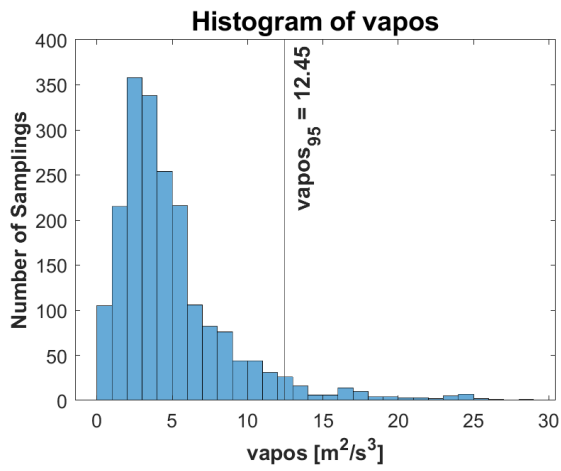
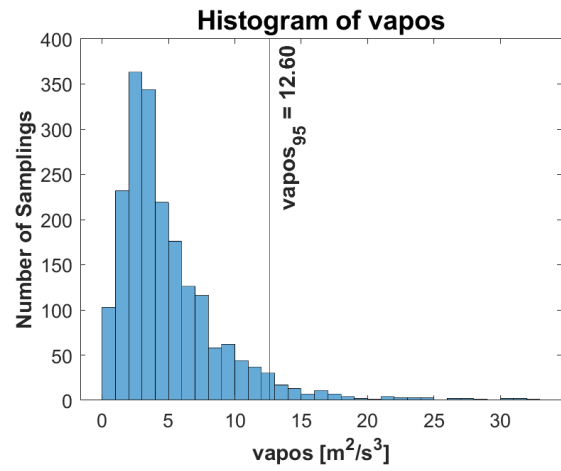


Figure A.13: PN Behaviour in Rural Section of Flat 1 Route for Same Speeds Between 2020 & 2018

A.6 Aggressiveness

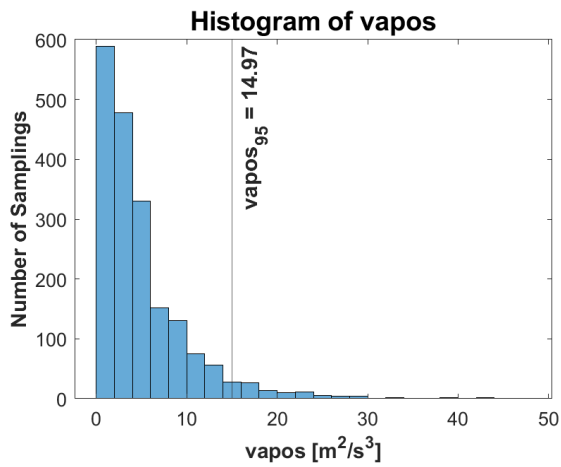


(a) Hilly 1

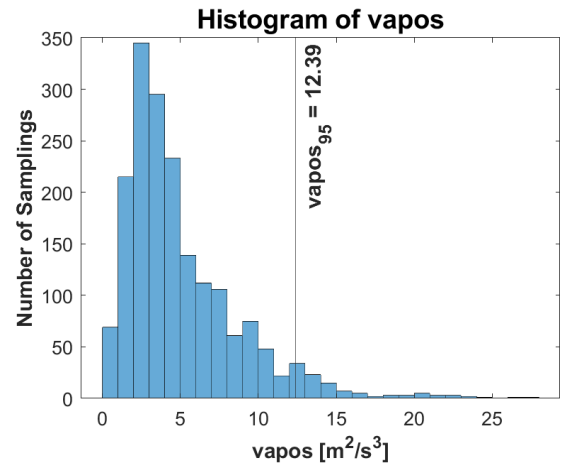


(b) Hilly 2

Figure A.14: Histogram of Aggressiveness ($vapos_{95}$) of Hilly Trips

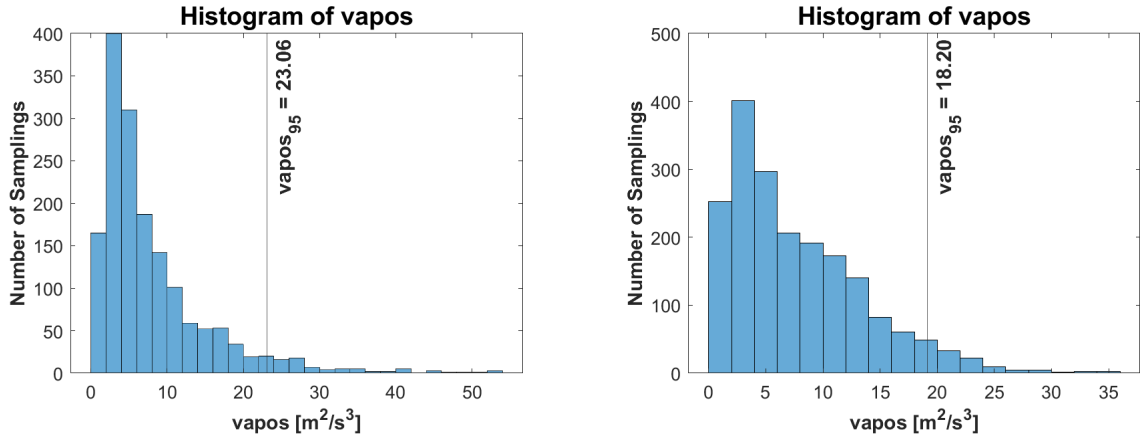


(a) Flat 1



(b) Flat 2

Figure A.15: Histogram of Aggressiveness ($vapos_{95}$) of Flat Trips



(a) Histogram of Aggressiveness (*vapos*) of In-cell AMHN

(b) Histogram of Aggressiveness (*vapos*) of In-cell FLHC 2

Figure A.16: Histogram of Aggressiveness (*vapos*) of In-cell

A.7 Additional Data

Table A.3: Average Coolant Temperature

Coolant Temperature [°C]						
Test	Flat 1	Flat 2	Hilly 1	Hilly 2	AMHN	FLHC 2
Urban	81.16	75.52	81.40	73.11	84.95	86.89
Rural	85.84	85.84	89.60	86.01	94.68	95.50
Motorway	81.83	85.71	89.82	84.50	98.52	99.41
Dif Urban	-5.73	-11.37	-3.55	-11.84	-	-
Dif Rural	-9.66	-9.66	-5.08	-8.67	-	-
Dif Motorway	-17.58	-13.70	-8.70	-14.02	-	-

A.8 Particle size distribution

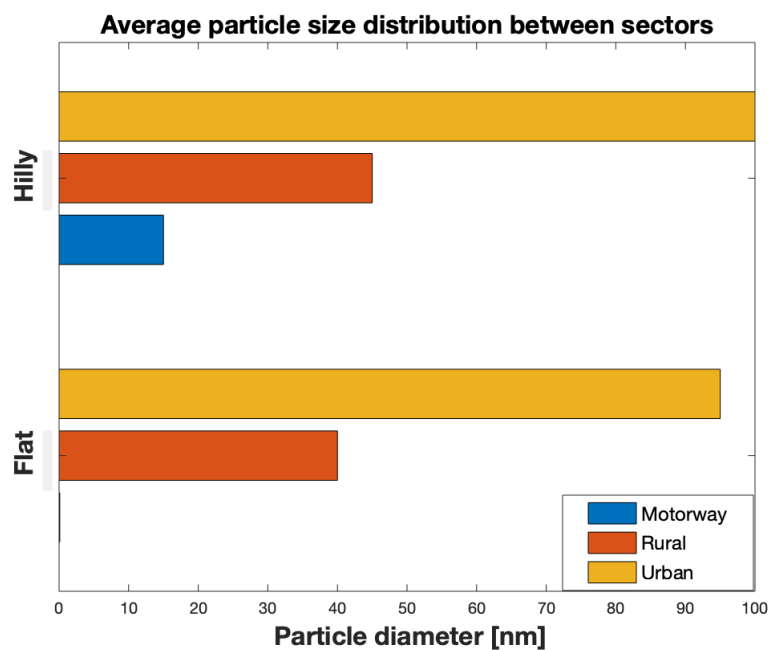


Figure A.17: Average particle size per trip section for Hilly and Flat cycles in test cell. Note - motorway section in flat shows zero only because test-29 failed to record that section.